NASA Contract Report 185164

Conceptual Design of Liquid Droplet Radiator Shuttle-Attached Experiment

Final Report

Shlomo L. Pfeiffer
Grumman Space Systems
Bethpage, New York

October 1989

Prepared for
Lewis Research Center
Under Contract NAS3-25357

CONTENTS

LIST OF FIGURES

LIST OF TABLES

1 – SUMMARY

The liquid droplet radiator (LDR) is an advanced heat rejection concept that shows the promise of radiating heat at a significantly reduced weight than current state-of-the-art heat rejection systems. The droplet radiator system works by generating thousands of submillimeter-sized droplets through space where the droplets radiate their heat. The droplets are collected via a positive displacement linear collection pump which recirculates the fluid back to the heat source.

The droplet generator system is acoustically driven and operates at a range of frequencies. The fluid used in this system is Dow Corning 704 silicone oil. Two different droplet collection schemes are compared: the centrifugal approach and the linear collection scheme. On the basis of simplicity, reliability, and weight, the linear collector method was selected for the conceptual design. The droplet loss detection system uses a moving laser beam coupled with a narrow field-of-view tracking detector to detect stray droplets.

The LDR experiment is estimated to weigh 73 kg (160 lb), be 9.1 m (30 ft) long, and fit within a 38.1 cm (15 in.) diameter. The experiment is designed to be integrated into the space shuttle bay using standard shuttle/experiment power, weight and data requirements.

2 – INTRODUCTION

It is anticipated that future space platforms will grow in size and will have an increasing need for lightweight, efficient waste heat removal systems. Presently, the heat rejection system can be the dominant weight in space platforms requiring more than a few hundred kilowatts of heat rejection. The LDR is an advanced heat rejection concept that shows the promise of rejecting large amounts of waste heat in a low weight and cost-effective manner.

A conceptual design of the LDR system is illustrated in Fig. 1. The waste heat fluid from the space platform is pumped to the LDR where it is generated into submillimeter droplets. The droplets radiatively cool as they pass through space from the droplet generators to the collectors. The cooled fluid is then recirculated back to the space platform.

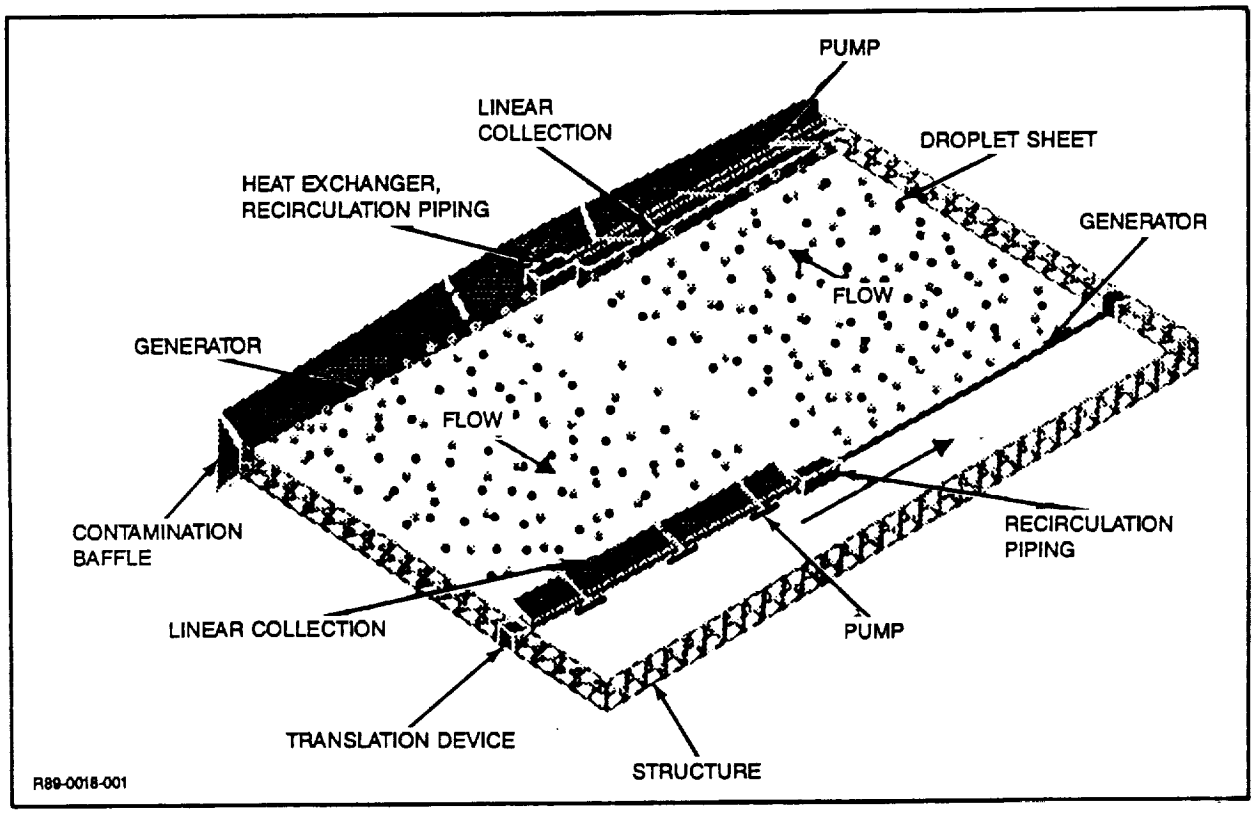

Fig. 1 Conceptual Design of LDR System

3 – BACKGROUND

The LDR concept was conceived in 1979. Several different LDR configurations were proposed, including spiral, enclosed disc, annular, and magnetic. These concepts are illustrated in Fig. 2. Currently the two LDR configurations which are considered the most viable, and which have been studied the most extensively, are the rectangular and triangular LDR systems (Fig. 3). NASA Lewis Research Center and the Air Force Astronautics Lab have been involved in funding and investigating many aspects of the development of these concepts.

Studies of the rectangular and triangular LDR concepts have been investigated by Grumman (Ref 1), the University of Washington (Ref 2), and McDonnell Douglas (Ref 3). Hardware fabrication and testing of the LDR generator and collector have been performed by several organizations including NASA Lewis, the University of Southern California, the University of Washington, Grumman, and McDonnell Douglas. Reference 4 gives a detailed background of the LDR issues, concepts, and developments that have been pursued to date.

Grumman has been involved in LDR development since 1984. Grumman built and tested a linear droplet collector with an integrated positive displacement pump (Ref 5). Additionally, Grumman has published results of analytical work characterizing LDR heat transfer considerations and droplet fluid dynamic behavior (Ref 1 and 7).

Potential Missions

Future NASA and Air Force heat rejection requirements will far exceed the heat rejection levels of current satellite systems. Table 1 lists possible future LDR applications and predicts their heat rejection requirements. Current state-of-the-art heat rejection systems such as heat pipe radiators weigh about 13 to 18 kg/kW (at ~300^{o}K) - excluding the weight of the interface mechanism. A high power space station may have a heat rejection requirement as high as 200 kW which translates into a 3500 kg (7700 lb) system weight for the radiators alone. Conversely, for the same heat rejection load, an LDR system would weigh about 500 kg (1100 lb) - including the weight of the generators, collectors, piping and supporting structure.

Reference 6 describes several advanced heat rejection concepts and reviews the suitability of these concepts to specific system requirements. The requirements include heat rejection load, weight, size, volume, launch loads and maneuverability. The results of the

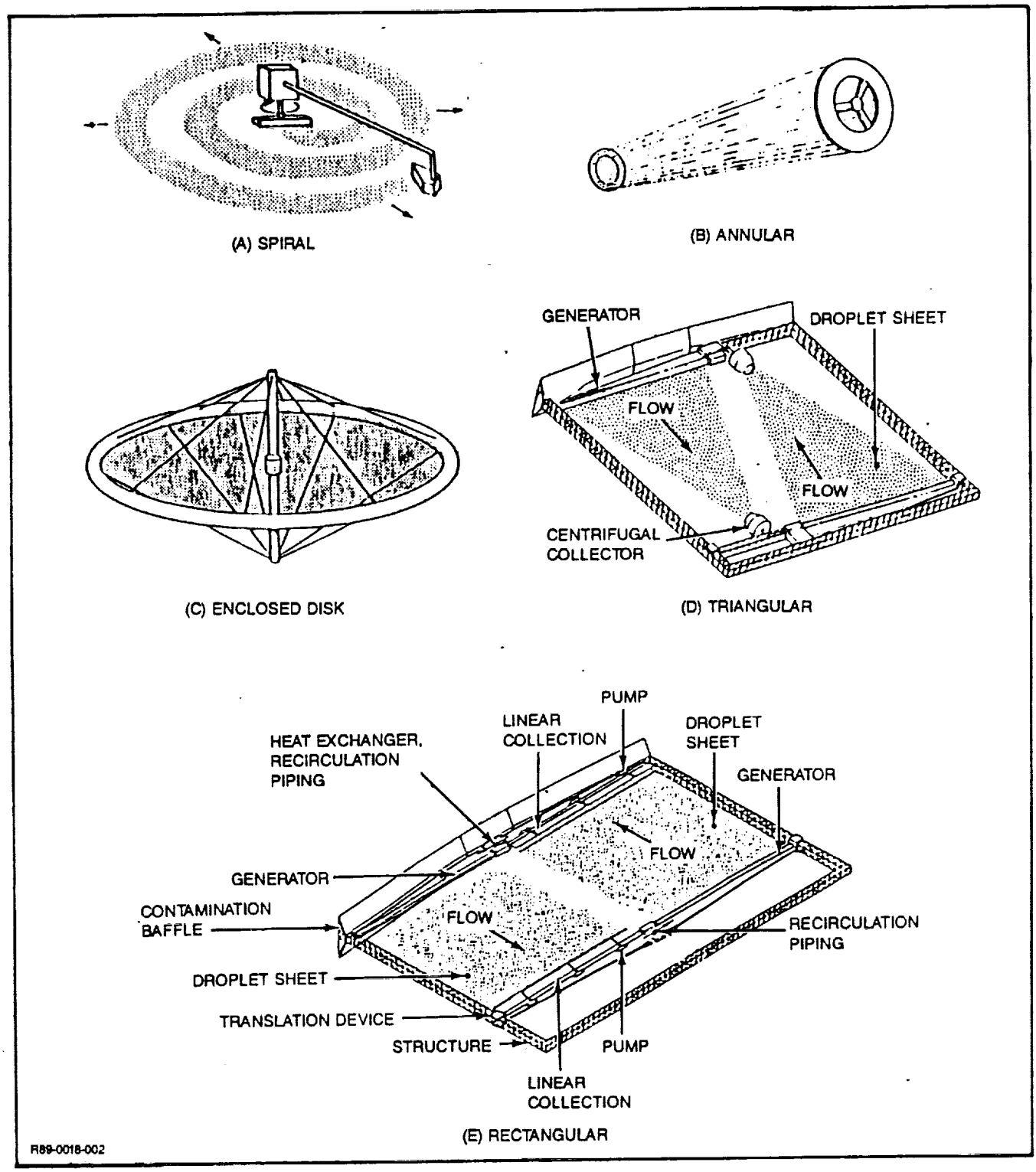

Fig. 2 Alternative LDR Concepts

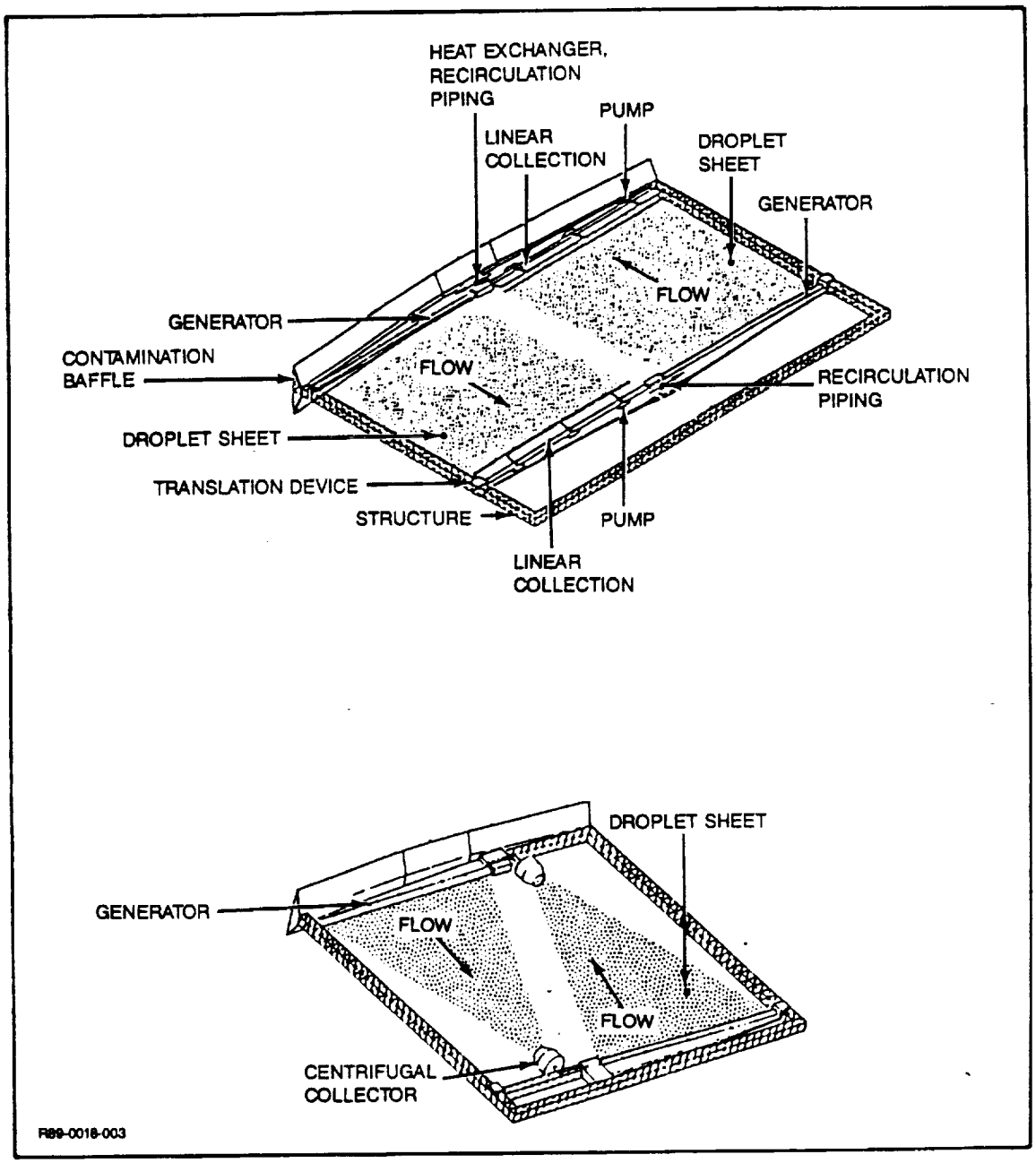

Fig. 3 Rectangular & Triangular LDR Configurations

Table 1 Potential Future Space Applications for LDR

Mission	Power Level	Duration
Future space station	75-300 kW	30 yr
Space-based lasers	1-10 MW	10 yr
Particle beam	1 MW	10 yr
Space-based radar	30-100 kW	10 yr
Lunar base	100-300 kW	30 yr
R89-0018-033		

study indicate clearly that for rejection temperatures below approximately 700°K, the LDR system is significantly lighter in weight than the other advanced radiator concepts. Figure 4 shows the LDR system weight in comparison to the heat pipe, curie point, moving belt, and rotating bubble membrane radiator system weights. Table 2 illustrates the relative weights of the various subsystems to the total heat rejection system weight for each concept.

To establish feasibility in a relevant environment, the LDR is proposed for a space flight test aboard the space shuttle. This document will discuss technical issues which the proposed experiment will address, show how the experiment will be integrated into the shuttle bay, detail the preliminary design of the experiment and estimate a cost and schedule for a follow-on LDR shuttle experiment development effort.

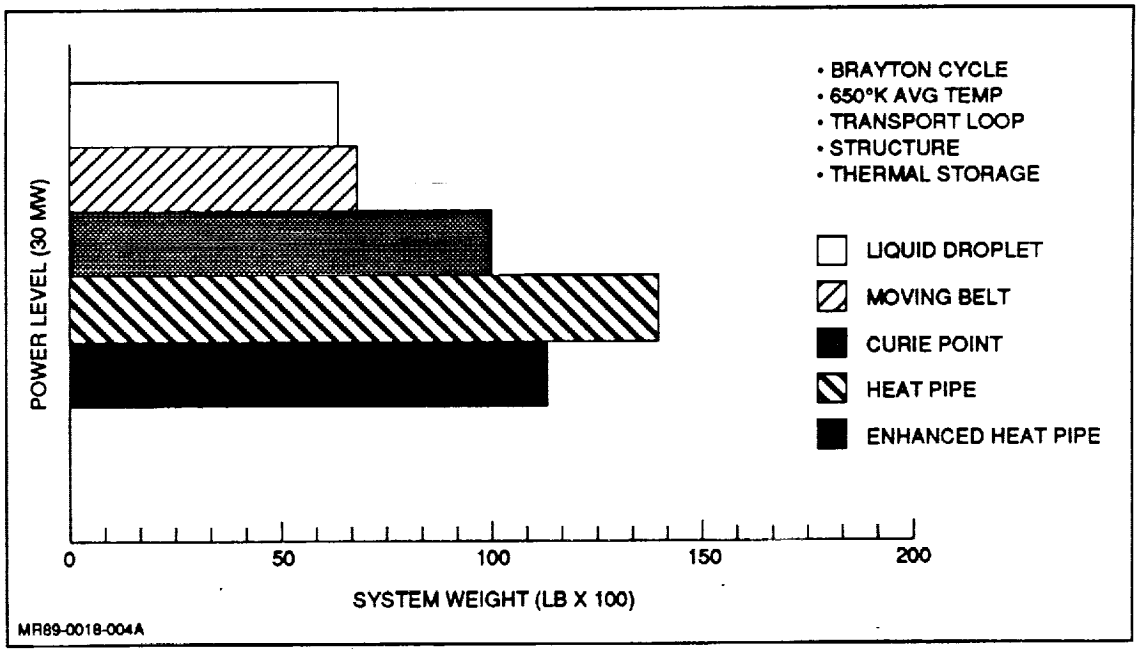

Fig. 4 Comparison of Advanced Heat Rejection System Weights

Table 2 Heat Rejection System Weight Summary

	Heat Pipe Radiator	Enhanced Heat Pipe Radiator	Liquid Droplet Radiator	Moving Belt Radiator	Curie Point Radiator	Rotating Bubble Membrane Radiator
Radiator	47,863	36,624	12,903	14,933	30,635	106,224
Structure	11,240	10,450	6,371	13,017	7,388	8,463
Transport Loop	1,484	1,484	7,008	2,607	4,400	1,796
TES	2,086	2,086	2,086	0	2,086	0
Other	0	0	211	0	0	0
Total	62,673	50,644	28,579	30,557	44,509	116,483
(Weights in kg)						
R89-0018-034						

4 – OBJECTIVES OF THE EXPERIMENT

The objective of the experiment is to investigate LDR-related physical phenomena that cannot be adequately tested or verified in a 1g or transient 0g environment and to demonstrate the operation of a fully integrated LDR system. The shuttle-attached experiment is designed to be integrated into the shuttle bay subject to the standard weight, power, data, and control constraints used for shuttle bay experiments. A layout of the LDR experiment is shown in Fig. 5. The experiment has a long aspect ratio - it is 9.1 m (30 ft) long and has a diameter of approximately 38.1 cm (15 in.). The droplet generator ejects thousands of droplets which are captured by a linear collector. Droplets which stray outside allowable limits are detected by the droplet loss detection system.

LDR heat transfer effectiveness is dependent on many variables. Droplet velocity, diameter, pitch and the number of droplet layers all contribute to the overall heat transfer

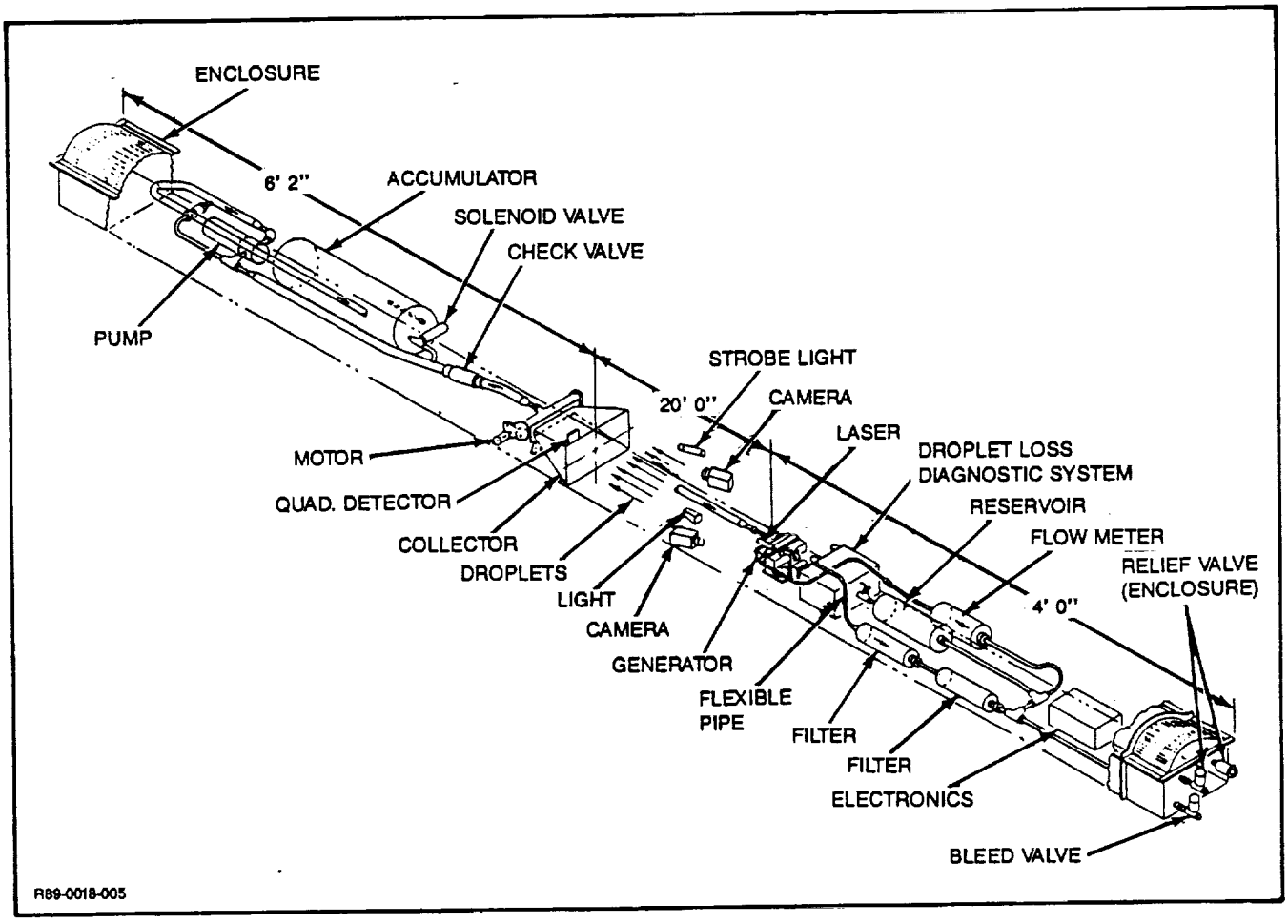

Fig. 5 LDR Droplet Radiator In-Flight Experiment

capability of the droplet sheet. Reference 1 details design considerations for maximizing the effectiveness of an LDR.

In order to assure that the shuttle-attached LDR experiment generates data that is applicable to future LDR applications, several 'full-up' LDR systems were investigated. One of the systems investigated was a future high-powered 200 kW space station. A trade study varying the number of droplet layers, droplet-to-droplet pitch and droplet velocity was conducted in order to determine factors which would decrease the weight of the system. As shown in Fig. 6, the minimum system weight occurs when the droplet sheet is limited to 20 layers. After that point, the advantage attendant with a higher sheet emittance is more than negated by the larger working fluid weight of the additional droplet layers. The LDR experiment was designed so that a representative subsection of a 'full-up' system could be investigated.

Below are listed the major issues which will be studied during the experiment. Those marked with an asterisk are issues that cannot be tested in a 1g environment or in the transient 0g environment of a KC-135 flight or a drop tower test:

- Startup
  - Generator start/stop performance*

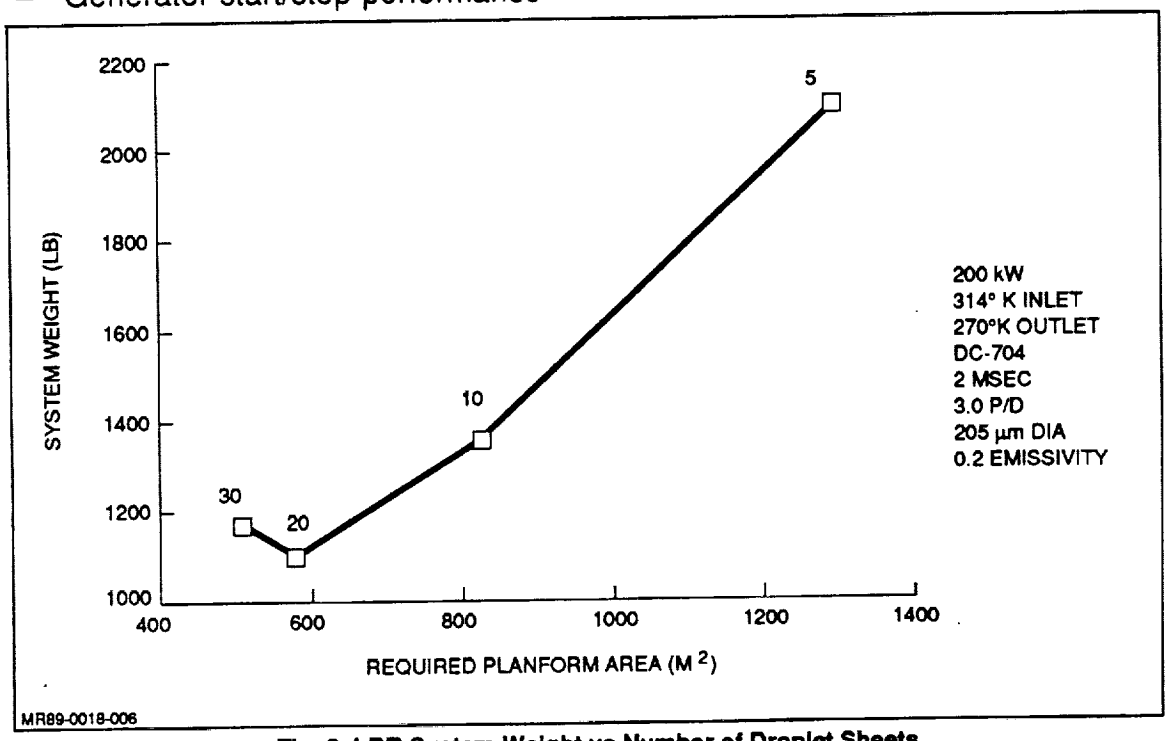

Fig. 6 LDR System Weight vs Number of Droplet Sheets

  - Generator surface wetting and droplet misalignment*
  - Establishing stable film flow on collector surfaces

- Steady run
  - Droplet stream characteristics
  - Droplet loss rate
  - Collector operation*
  - Boost pump operation
  - Droplet heat transfer characteristics
  - Fluid backflow from collector surface*
- Shutdown
  - Effect of fluid decay on collector operation*
  - Generator shear seal operation*

In addition to the aforementioned issues, one of the objectives of the experiment will be the demonstration of the manufacturability of an orifice plate with several thousand holes which can achieve less than 5-mrad parallelism. The experiment will, of course, serve to allay fears of potential LDR users regarding droplet loss and spacecraft contamination.

5 – EXPERIMENT DEFINITION

Overview

A schematic of the LDR experiment is shown in Fig. 7. Dow Corning 704 silicone oil is stored in a rectangular cavity with a single transducer as a cavity wall opposite the plane of the jets. The transducer oscillates between 4 - 30 kHz to generate droplets at velocities between 2 - 10 msec. The fluid is forced through the orifice plate which contains 4000 orifices, each of which are 100 μm in diameter. The orifice plate must be manufactured to achieve a droplet divergence of less than 5 mrad. The droplet generation must be stable and repeatable so that heat rejection requirements will be fulfilled. As the droplets travel from the generator to the collector, the droplet loss detection system will count the number of stray droplets and calculate their velocity and position. The droplets will be detected by reflections from a pair of scanning laser beams which oscillate around the perimeter of the droplet streams.

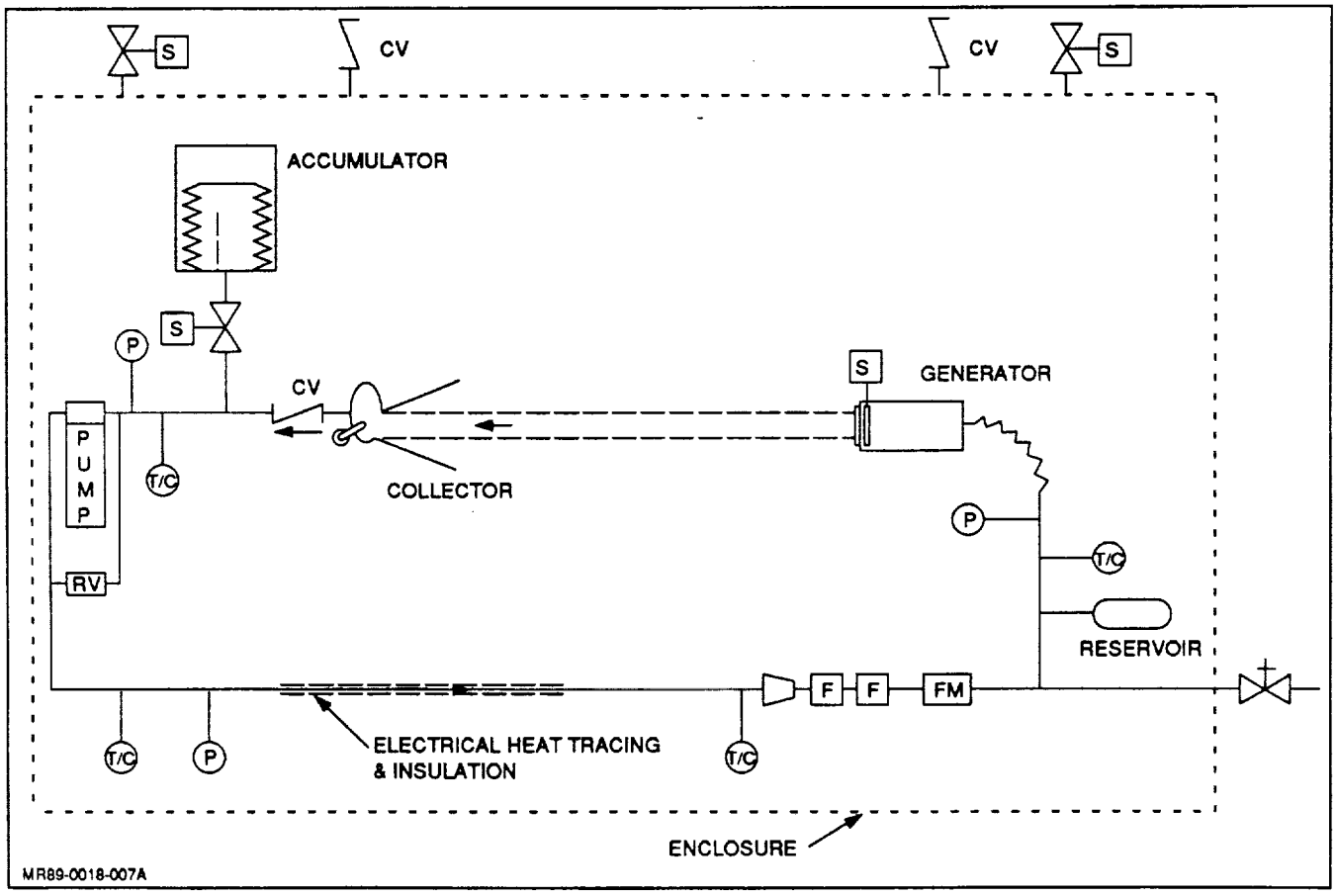

Fig. 7 Schematic of Experiment

The droplet collector is a wide throat positive displacement gear pump. The width of the collector module is slightly larger than the generator. The fluid from the droplet streams is collected in the throat of the collector and is forced into the gears by the pressure of the droplet streams on the back side of the collected fluid. An isometric view of the collector is shown in Fig. 8. The pump shown is representative of what a collector pump on a 'full-up' system would look like.

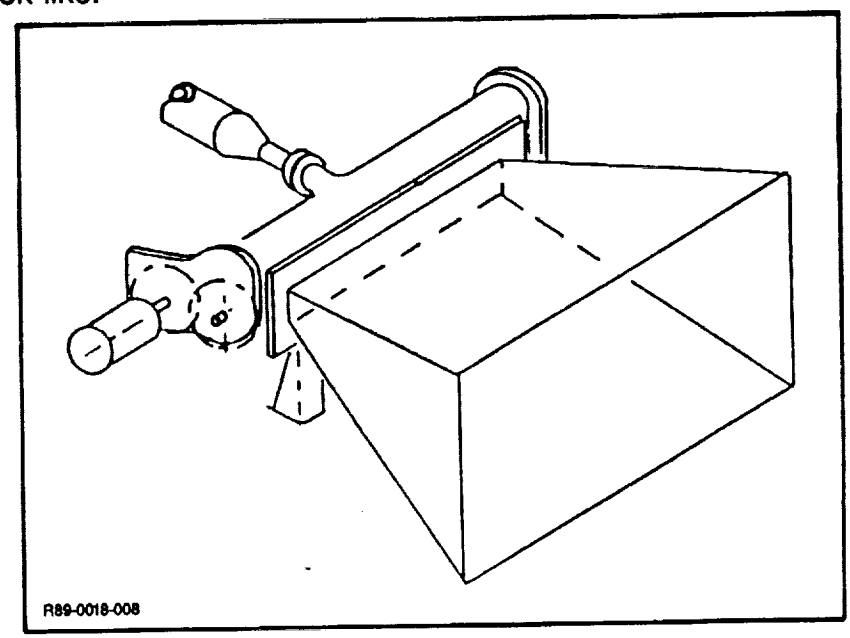

Fig. 8 Isometric View of Collector

After the fluid is discharged from the collector pump it goes into the high pressure boost pump which will boost the fluid up to the pressures required for proper droplet formation at the generator. The experiment will be run at droplet velocities of 2, 4, 7, and 10 msec. Data will be collected at these velocities in order to measure the effect of the different droplet velocities on collector/generator performance.

Generator

Figure 9 details the design of the LDR generator. The generator is equipped with a laser alignment system which determines if the droplet spray from the generator is directed into the mouth of the collector. Motorized positioners rotate the generator about two axes in order to correct for any misalignment due to structural deformations. The generator fluid cavity is designed so that the generator can eject droplets with velocities ranging from 2 to 10 msec. The droplets are acoustically generated by a piezoelectrically-driven transducer operating at set frequencies. The rectangular cavity is designed to provide a sufficient pressure perturbation at four nominal droplet velocities.

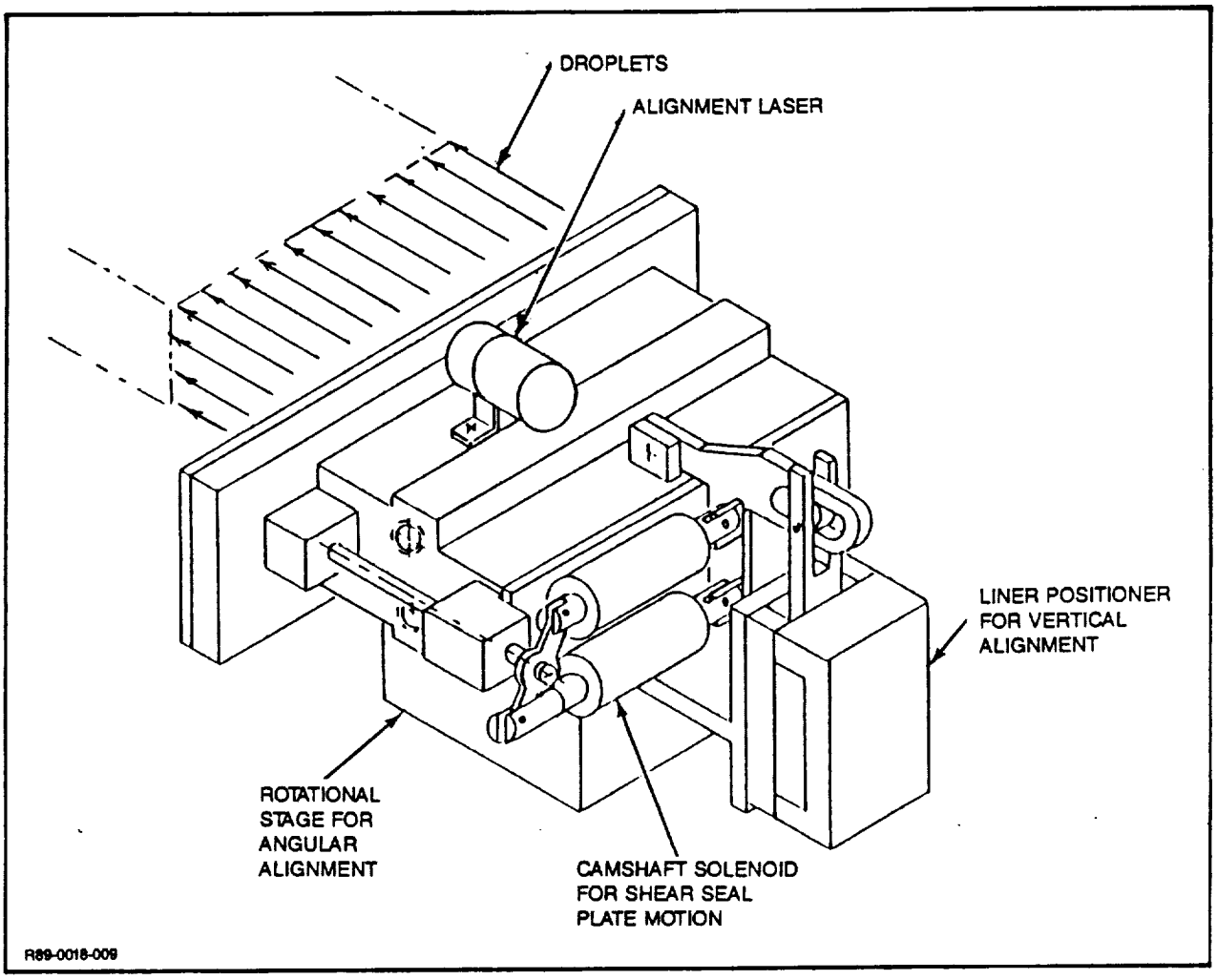

Fig. 9 Droplet Generator

A major factor in the design of the generator is the startup and shutdown of the droplet streams; Fig. 10 illustrates a schematic of the Grumman shear seal design. A push-pull solenoid valve turns a camshaft which slides the shear seal into either the opened or closed position. In order to be effective, the shear seal mechanism must be actuated in the millisecond time frame.

Performance Criteria

The performance criteria for an LDR shuttle experiment drop generator are as follows:

- Clean Start /Stop - The drop generator is one of many components in the system used to start and stop the droplet sheet. Start/stop performance acts as a constraint on the design of the drop generator in that the drop generator design must not make achievement of good start/stop performance difficult or impossible

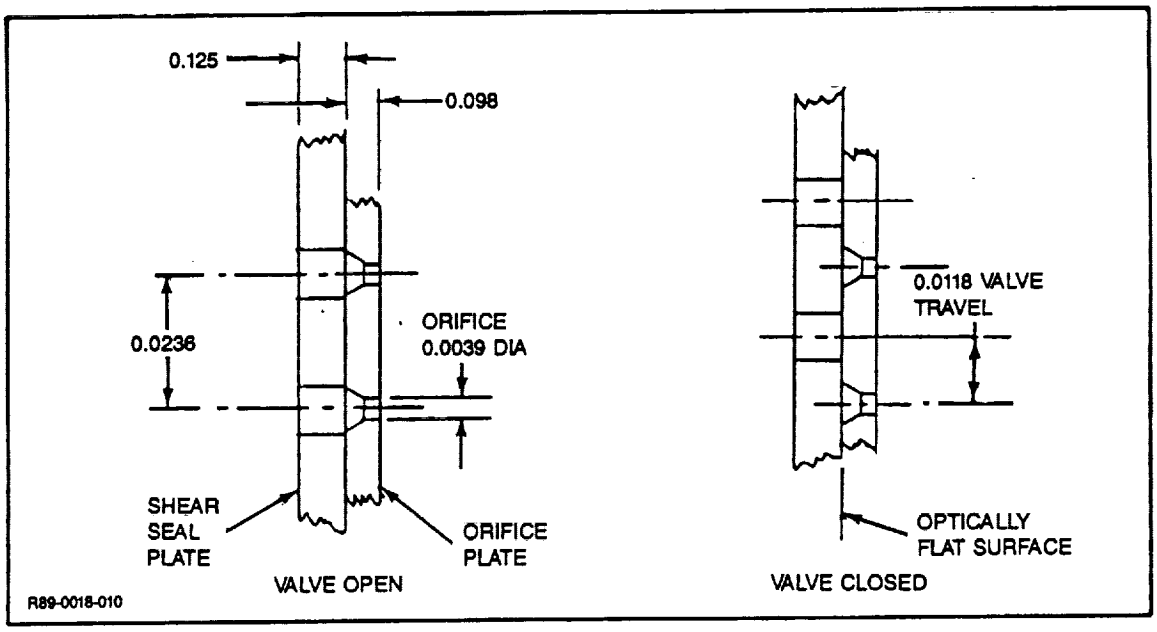

Fig. 10 Shear Seal Valve

The specifics of this requirement in turn depend on the start/stop method employed. For instance, if the drop generator is normally at ambient pressure and an upstream valve is used to deliver fluid under pressure to the drop generator, then the drop generator hydraulic compliance (i.e., fluid volume and structural compliance) and flow resistance must be minimized to achieve a sharp pressure rise during startup (and fall during shutdown) in the drop generator. Rapid rise and fall time of the pressure are the key requirements for clean start/stop

- If a shear seal valve is used to actuate the jets, then the hydraulic compliance of the drop generator cannot be too low. This would cause the pressure in the drop generator to drop after the initial actuation of the jets The pressure would remain low until the source pressure propagates to the drop generator. This pressure drop would cause the jets to wander and possibly stop momentarily. Drop generator flow resistance must also be low in a shear seal start/stop system

- Straight Jets - The requirement for straight jets is the most obvious requirement for the drop generator. This is principally a requirement on the orifice plate and its fabrication, but jet straightness is influenced by fluid properties, jet operating parameters, and drop generator structural behavior (Ref 9). The current requirement for jet straightness for the LDR is all jets less than 5 mrad

- Drop Generation - For a LDR to reject heat as designed, the droplet generator must produce stable drops of the proper size and with proper velocity. Drop generation performance will be a function of fluid properties, jet operating parameters, orifice quality and diameter, and design of the pressure perturbation generator (referred to as the stimulator)

  Two LDR design issues involve (1) off design (i.e., low heat rejection rate) operation and (2) selection of optimum operating conditions from the conflicting areas of heat transfer efficiency and drop generation efficiency. In order to provide information to resolve these issues, the LDR shuttle experiment will be required to operate at four significantly different jet velocities, each using the frequency for optimum drop formation for that velocity.

Critical Components

From the above discussion of the performance criteria of the drop generator, its critical components may be derived:

- Orifice plate
- Jet flow/stimulator operating conditions
- Stimulator.

Orifice Plate

The requirements for generation of droplets in an LDR are in most cases a subset of the performance criteria for a continuous ink-jet printing system of 880 orifices. Development of orifice plate fabrication technology is being investigated by MicroFab under contract with NASA Lewis (Ref 9).

The drop generator in the LDR shuttle experiment must have an orifice plate with a significant number of orifices. It would also be useful if the number of orifices represented a reasonable LDR sub-unit size. To allow performance of an LDR to degrade gracefully due to failure of a single or small number of orifices (e.g., due to contamination of an orifice), an operational LDR drop generator will be broken up into sub-units of approximately 1% of the total array size.

Several optimization studies (Ref 4, 5, 10, and 11) have examined the optimum LDR operating conditions for several different applications. These operating conditions determine the required orifice diameter for the LDR drop generator. Based on a relatively low temperature (300^{o}K) heat rejection application, an orifice diameter of 100 μm was selected.

The optimization studies cited in the above paragraph have also examined the configuration of the orifice plate, i.e., what are the optimum number of rows in the droplet sheet. These studies showed that for a 300^{o}K system above 20 rows, the weight increases faster than the heat transfer rate. Therefore the 4000 orifices selected above will be arranged in a 20 by 200 configuration.

Orifice-to-orifice pitch is a compromise between manufacturability (easier at higher pitches) and performance (weight and size less, strength greater at lower pitches, see Ref 9). As a compromise, a pitch-to-diameter of six was selected. This results in a pitch of 600 μm and a total array size of 0.012 m by 0.119 m.

The type of orifice plate to be employed in the shuttle experiment has not yet been firmly established. On the basis of previous experience, electroforming was selected as the orifice fabrication technology that will be used for the orifice plate for the shuttle-attached experiment. The orifice plate fabrication method determines the shape of the orifice/nozzle and the thickness of the orifice plate. These in turn affect the jet operating parameters and the structural design.

Working Fluid & Operating Temperature

For the low temperature (300^{o}K) heat rejection applications, low vapor pressure silicone oils have been deemed acceptable. In particular, Dow Corning 705 silicone oil has a very low vapor pressure and is thus best suited for long duration mission requirements. For the duration of the shuttle LDR experiment, Dow Corning 704 was selected as the working fluid because it would give equivalent performance at a substantially lower cost.

To simplify the design and increase reliability of the experiment, it was decided to allow the experiment to operate at ambient shuttle bay conditions. To avoid operating at the lower temperature end of possible bay ambient temperatures, a heater is included in the fluid system maintain the fluid at a minimum of 25^{o}C. Thus the operating temperature range for

the fluid in the experiment is 25 - 37.7°C. The resulting fluid properties of Dow Corning 704 are thus:

Density,	ρ	$= 1070\ kg/m^3$
Surface tension,	σ	$= 0.0365\ N/m$
Kinematic viscosity,	ν	$= 39 \times 10^{-6}\ m^2/sec$ at 25°C
		$= 22 \times 10^{-6}\ m^2/sec$ at 37.7°C

Jet Operating Parameters

After several iterations, a nominal design orifice flow velocity of 4 msec was selected. This represents a compromise between the desire for low velocities for optimum heat transfer performance and the need to operate the jets at a high enough Weber number that surface tension does not cause jet straightness and start/stop problems. Off-design orifice flow velocities of 2, 7, and 10 msec were selected. The resulting mass flow, volume flow, and Weber numbers are shown in Table 3.

In general, the jet velocity and mean orifice velocity are not usually the same (Ref 12,13), in part because the jet and orifice diameters can differ (Fig. 11). To simplify the analysis (explicit equations vs implicit ones), the average orifice velocity, or flow rate, was chosen as the primary variable. Assuming a fully developed velocity profile at the exit of the orifice, the data and analysis of Ref 12 and 13 were used to determine the contraction coefficient ($C_c = A_{jet}/A_{orf} = \{d_{jet}/d_{orf}\}^2 = V_{jet}/V_{orf}$) for each of the four V_{orf} cases at both the high and low operating temperatures. This in turn was used to determine the jet velocity and diameter for each case. These values are given in Tables 4 and 5. Note that the asymptotic value of C_c for a fully developed exit profile as $Re \rightarrow \infty$ (no surface tension) is 0.69. (Ref 5 and 13).

Table 3 Jet Parameters Independent of Temperature

Case	V_{orf} (msec)	Q, 4000 jets (m^3/sec)	m, 4000 jets (kg/sec)	We_d	Frequency (kHz)
1	2.0	6.2 x 10	0.067	12	4
2	4.0	1.3×10^{-4}	0.134	47	10
3	7.0	2.3×10^{-4}	0.235	144	20
4	10.0	3.2×10^{-4}	0.337	293	30

R89-0018-035

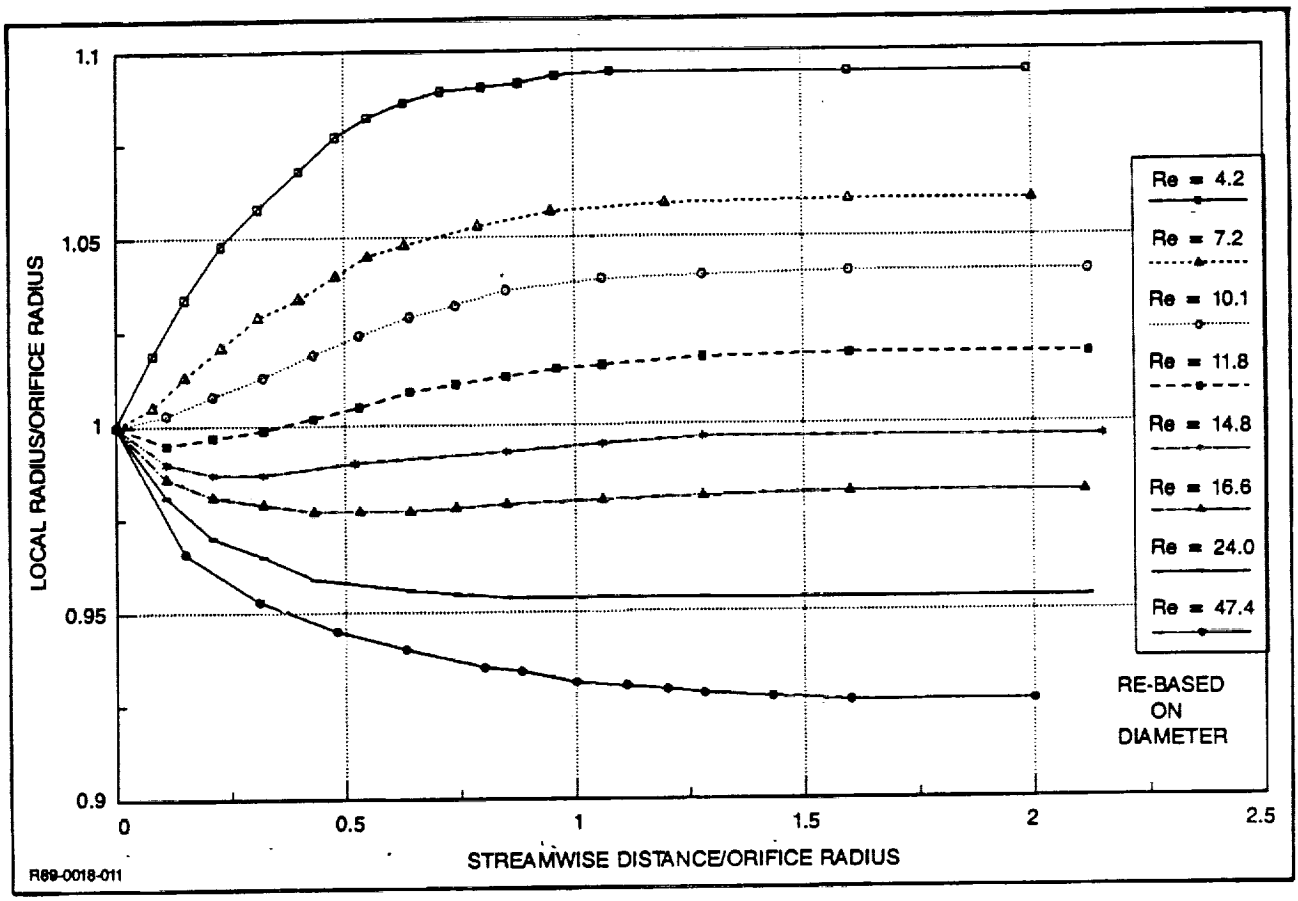

Fig. 11 Jet Diameter vs Reynolds Number

To determine stimulator frequency and drop size, the wavelength of the disturbance applied to the jet, l, was chosen so that l/djet = 4.0. From a heat transfer standpoint, it is desirable to minimize l/djet, but the nominal value selected must be greater than the theoretical minimum of 3.0 (Fig. 12) by an amount sufficient to allow all of the jets in the array to have l/d_{jet} greater than 3.0.This is a good example of the tradeoffs and compromises that must be made in an array design. The principle cause of variation in l/djet across the array will be orifice diameter variation. To desensitize the system to orifice diameter variations of a certain magnitude, the nominal l/djet selected must be significantly greater than the minimum. If lower values of /djet are desired, the allowable variation in orifice diameter would have to decrease.

Using λ/d_{jet} = 4.0, the operating frequency of the array and the resulting drop diameter were computed and these are shown in Table 4 and 5.

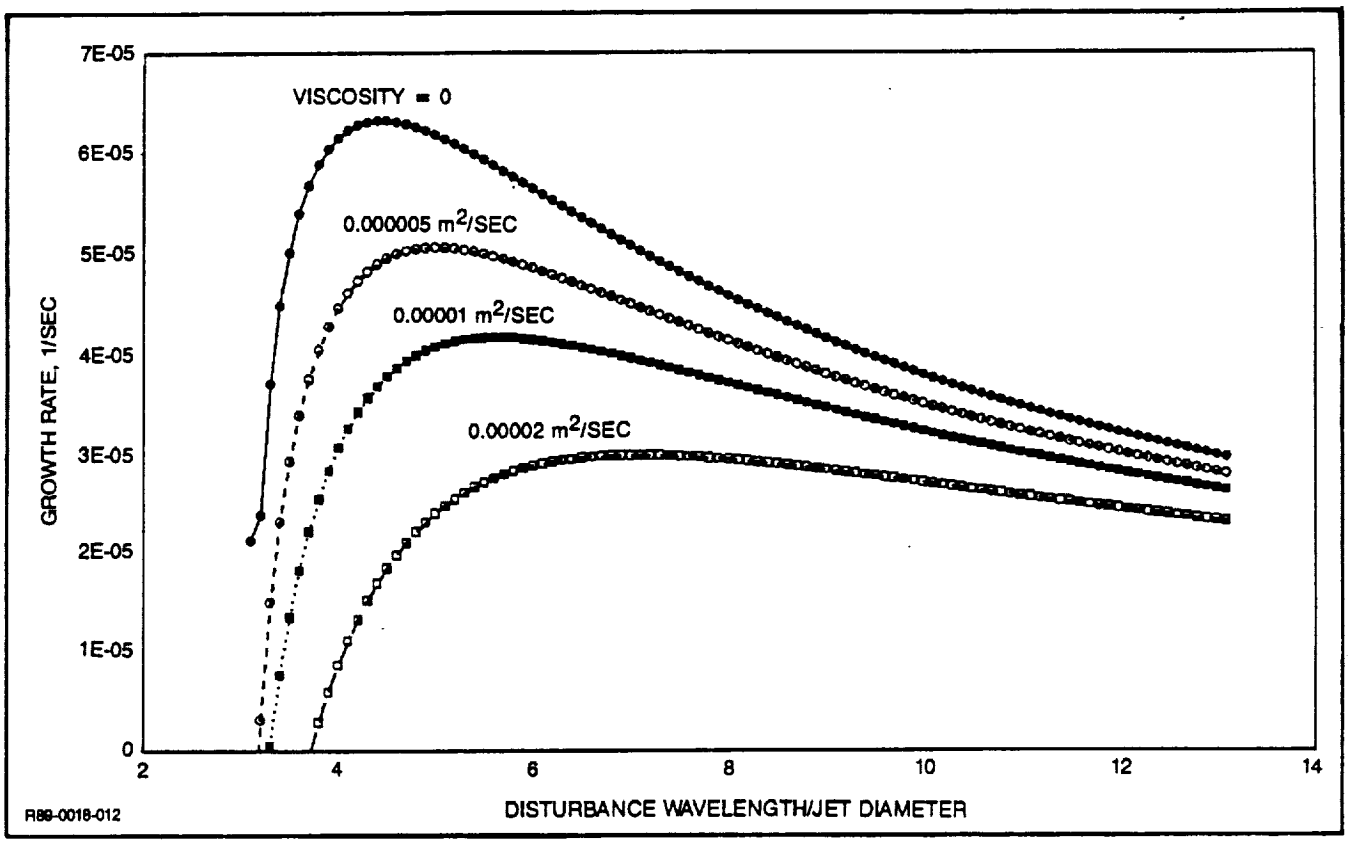

Fig. 12 Disturbance Growth Rate for a Capillary Jet

Table 4 Jet Parameters at T_{min} = 25° C, λ/d_{jet} = 4

Case	R_d	C_c	d_{jet} (μm)	V_{jet} (msec)	Frequency (kHz)	d_{drop} (μm)	Pressure (kPa, psi)
1	5.1	1.19	109	1.7	3.9	187	87, 12.7
2	10.2	1.06	103	3.8	9.2	187	180, 26.2
3	17.9	0.94	97	7.4	19.1	177	333, 48.4
4	25.5	0.90	95	11.1	29.2	173	500, 72.6

R89-0018-036

Table 5 Jet Parameters at T_{max} = 37.7° C, λ/d_{jet} = 4

Case	R_d	C_c	d_{jet} (μm)	V_{jet} (msec)	Frequency (kHz)	d_{drop} (μm)	Pressure (kPa, psi)
1	9.1	1.10	105	1.8	4.3	191	50, 7.3
2	18.2	0.94	97	4.3	11.0	177	106, 15.5
3	31.9	0.88	94	8.0	21.3	171	204, 29.6
4	45.5	0.83	91	12.1	33.2	166	315, 45.8

R89-0018-037

To calculate the required pressure for each of the four orifice velocity cases at the high and low operating temperatures, the following model was used (Ref 14,15, and 16):

$$C_p = K+K'/Re_d+ (32/Re_d) (L/d_{orf})+4/We_d$$

where,

C = the pressure loss coefficient

p = $\Delta P/(\rho V^2_{orf}/2)$, or actual to ideal pressure drop through the orifice

ΔP = the manifold total pressure minus the atmospheric pressure

K = the Hagenbach coefficient that represents both the required energy to accelerate the jet to V_{orf} (K=1) and any entry flow loss that is not a function of Reynolds number (K>1)

K' = the Couette coefficient that reflects Reynolds number dependent entry flow loss

Re = Reynolds number based on orifice flow parameters, d_{orf} and V_{orf}

We = Weber number based on orifice flow parameters, d_{orf} and V_{orf}

L/d_{orf} = length to diameter ratio of the orifice/nozzle

Note that pressure drop calculations in some LDR references (Ref 5 and 17) include only the fully developed flow (third) term and thus consistently underestimate the required pressure. For liquid metal flows, omission of these terms would give required pressure values that are drastically low due to the high Reynolds numbers associated with these flows.

The values of K and K' were taken as 1.5 and 200 (Ref 18). For the electroformed orifice plate selected, there is no constant area section, so $L/d_{orf} = 0$. The pressure drop equation was used for each of the four orifice flow cases at both the high and low operating temperatures. These results are also shown in Tables 4 and 5.

Stimulator

To cause a jet to break up into a stream of uniform drops, a disturbance in the radius of the jet must be created and its frequency must be within certain limits. The components of the drop generator that create and transmit this disturbance are referred to as the stimulator. A wide variety of stimulation methods have been demonstrated in commercial and laboratory systems. In a conventional continuous array ink jet printer, the performance criteria for the stimulator are the establishment of satellite free operation for every jet, break-off length within some bandwidth for every jet, and the phase angle within 90 deg for every jet. An LDR requires only that the drops be the correct size and velocity and be stable.

Systems that try to decouple the stimulation from the fluid path generally attempt to create a motion of the drop generator structure. Many different methods and designs have been successfully employed, but they all produce the same net effect: a surface that is normal to the direction of flow, usually the orifice plate itself, is caused to move parallel to the direction of flow. This creates a pressure perturbation that results in a jet diameter perturbation. Structurally induced drop generations have several advantages: fluid cavity shape and size restrictions are relaxed; the motion inducing components, usually piezoelectric materials, do not have to be compatible with the fluid; the stimulator does not have to be sealed from, while at the same time coupled to, the fluid; and there's no need to guard against the shedding of particles from the stimulator.

Structurally induced stimulation methods are restricted by the combination of frequency, materials properties, and dimensions of the drop generator. The lower the operating frequency and the smaller the drop generator, the easier it is to utilize a structurally induced stimulator.

Another type of drop generator design, referred to as acoustic stimulation, attempts to couple the motion of the transducer directly to the fluid and not to the structure. This type of stimulator can be very efficient since the energy is transmitted directly to the fluid. The analysis of an acoustic stimulator is fairly straightforward. This is important for the LDR experiment due to the desire to operate at four drastically different frequencies. Because acoustic stimulation was judged to be the most conservative approach, it was selected for the LDR shuttle experiment drop generator.

Acoustic Cavity

A rectangular cavity with a single large transducer as a cavity wall opposite the plane of the jets was selected for evaluation. See Fig. 13 for a description of the configuration. A rectangular cavity was selected both for ease of analysis and because a multiple row orifice array does not allow much design latitude for a trapezoidal cavity, which would be more efficient.

The performance criterion of the acoustic cavity is to provide a sufficient level of disturbance (i.e., pressure perturbation) to all of the jets at the four nominal frequencies given above. At the same time, the cavity dimensions should be kept to a minimum in order to minimize size and weight. This is further constrained by the fact that the minimum of two of

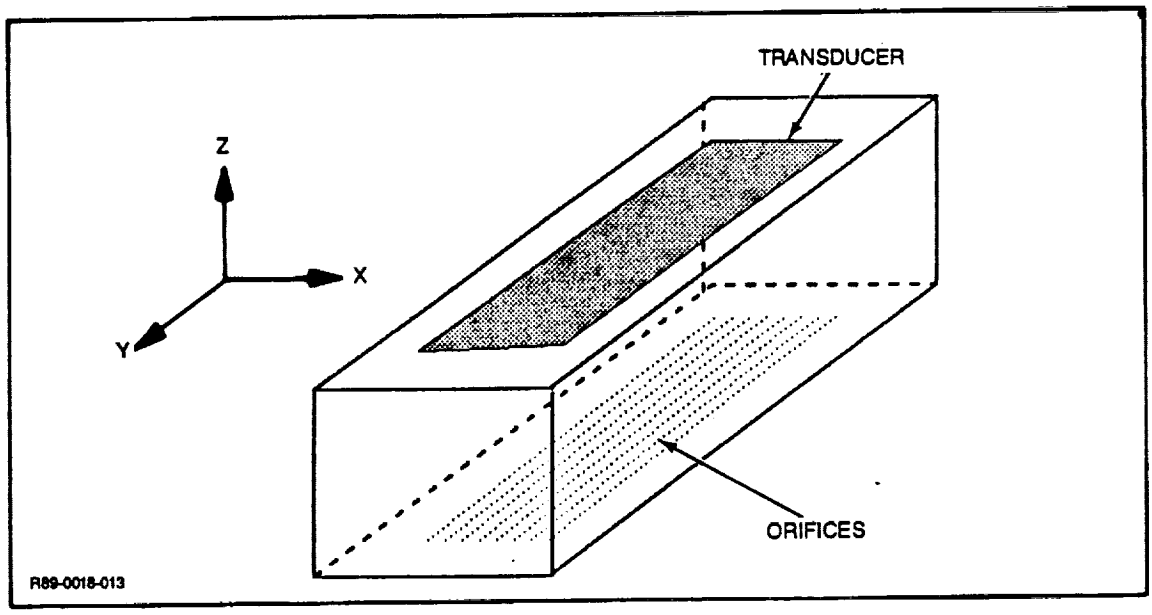

Fig. 13 Acoustic Cavity Configuration

the dimensions of the acoustic cavity are determined by the orifice plate length and width. This in turn determines the maximum resonant frequencies for two of the three primary modes.

A closed form solution for a driven rectangular cavity with rigid walls is known (Ref 19), and the equation for the pressure field from Ref 19 was programmed to calculate the pressure at each orifice as a function of cavity geometry, driver geometry, orifice location, fluid properties, and frequency. The pressure perturbation supplied to the orifices was then examined as a function of cavity geometry at the four nominal frequencies.

The design guideline for cavity height is given as follows: the height (normal to the orifice plate) should be slightly less than half the acoustic wavelength. Since this is obviously a fixed frequency criterion, one of the nominal frequencies must be selected in order to determine the wavelength. Configurations using both the 10 and 20 kHz values to determine the wavelength were examined. Using 10 kHz to determine the wavelength resulted in the widest operating frequency range.

With the cavity height fixed, the other two dimensions were varied to optimize performance. The design objective for these dimensions is to avoid lengths that are integer multiples of the wavelength(s). The final resulting acoustic cavity dimensions were as follows: Lx = 0.014 m; Ly = 0.121 m; Lz = 0.070 m; Px = 0.10 m; Py = 0.121 m, where the L's are cavity dimensions and the P's are transducer dimensions. The pressure distributions for

the final cavity geometry at the four nominal frequencies are given in Fig. 14 - 16 (the "0" value in the figures represent the center of the array). The figures show that operation at 10 and 20 kHz should produce sufficiently uniform pressure perturbations across the array. Operation at 4 and 30 kHz may result in regions of the array being under driven. To determine the absolute level of performance, the transducer performance must be estimated.

Transducer

In the above analysis, the transducer was unspecified. A bender type will be used because of its simplicity and performance capability. This type of transducer uses a flat, thin piezoelecric crystal bonded to a flat, stiff member, usually metal. The piezoelectric material is poled in the thin dimension and when a voltage is applied across it, a shear force at the interface of the two materials causes a bending moment, which in turn causes the transducer to deflect. The general concept of a bender configuration is shown in Fig. 17.

Using an analysis program previously developed at MicroFab, the performance characteristics of a piezoelectric crystal/metal bimorph driving a fluid were analyzed. This program makes the following assumptions: radial geometry, simply supported ends, single event transient (i.e., not periodic), and simple wave flow. The first assumption makes the results conservative and the second and last make them optimistic.

In addition to the above assumptions, the following were used in the analysis: piezoelectric material - PZT-5H (Vernitron product name), metal - stainless steel, drive frequency - 10 kHz (i.e., rise and fall time = 25 msec); maximum voltage - 100 V. The latter was chosen as a practical system limit and for the thickness selected will be far below the maximum voltage that PZT-5H can take.

The principal design requirement for the transducer is that it produce sufficient motion for the case of simple wave flow, with the constraint that the structural resonant frequency be greater than the highest operating frequency, 30 kHz. This criterion is required for the separate analyses of the transducer and cavity to have meaning. Using a transducer with a resonant frequency of 10 kHz might make for a functional design, but the analysis required to verify its performance is difficult. In addition, it would result in a much thinner transducer which could be incompatible with the 500 kPa (70 psi) maximum pressure.

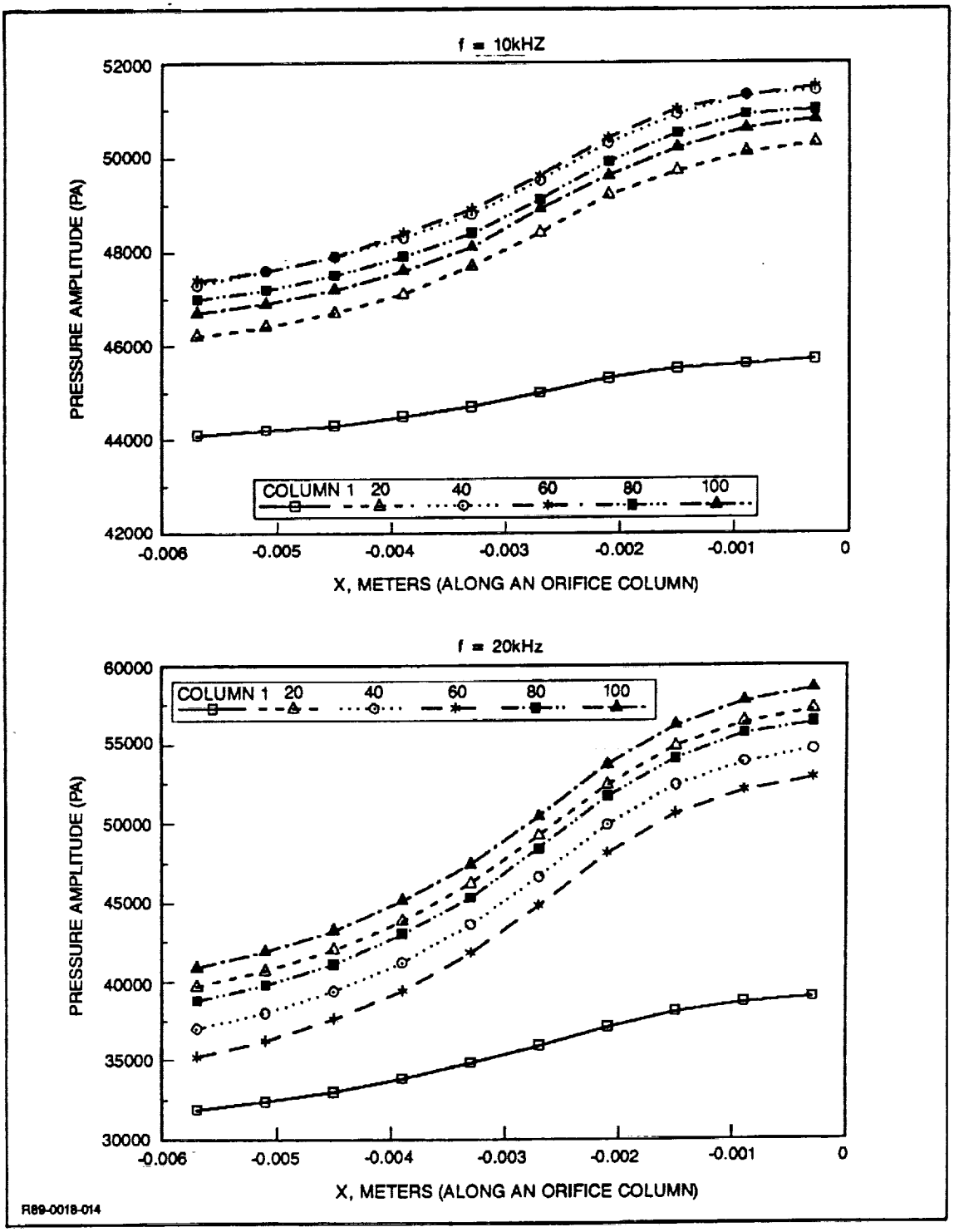

Fig. 14 Acoustic Cavity Pressure Distributions, f = 10 & 20 kHz

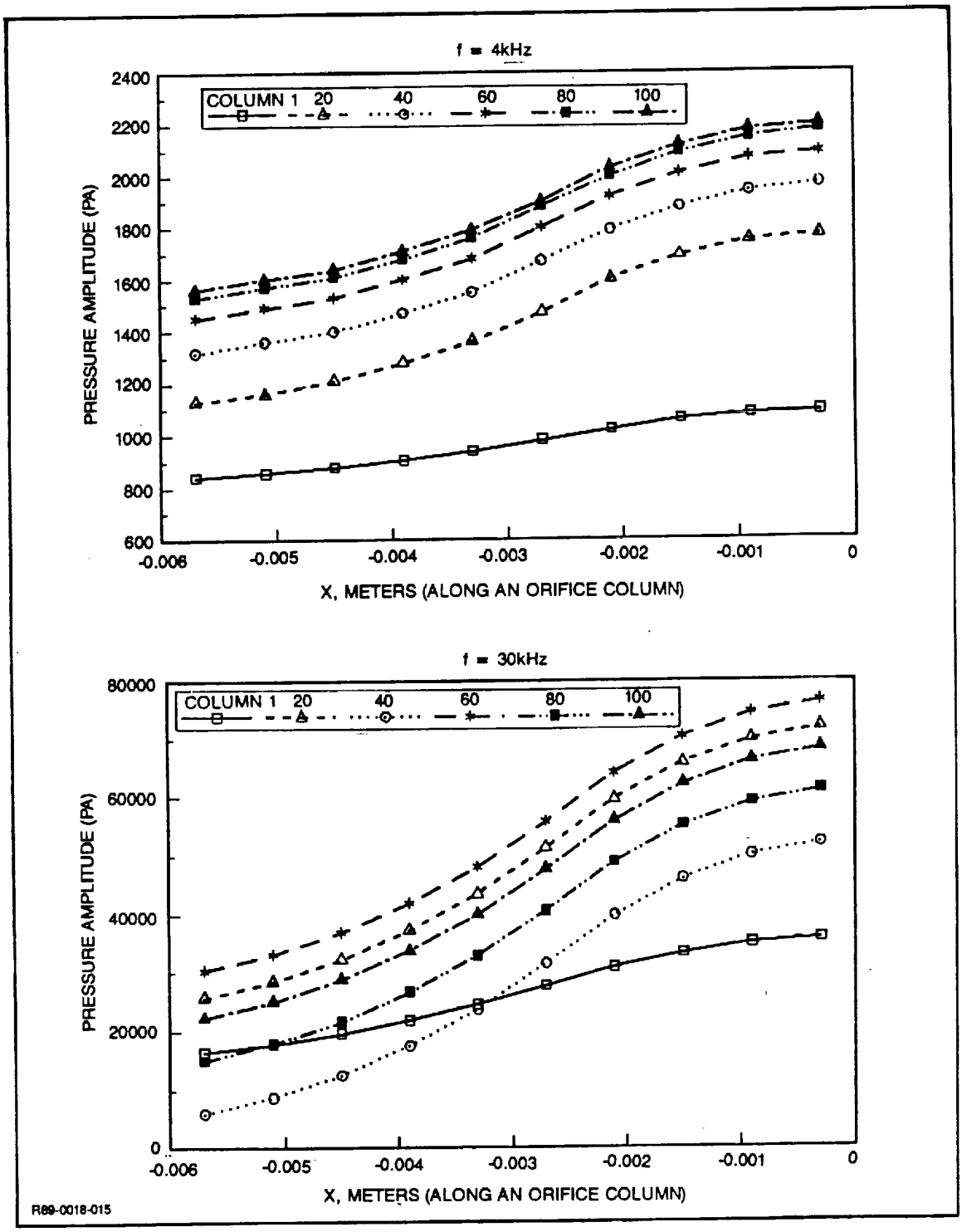

Fig. 15 Acoustic Cavity Pressure Distributions, f = 4 & 30 kHz

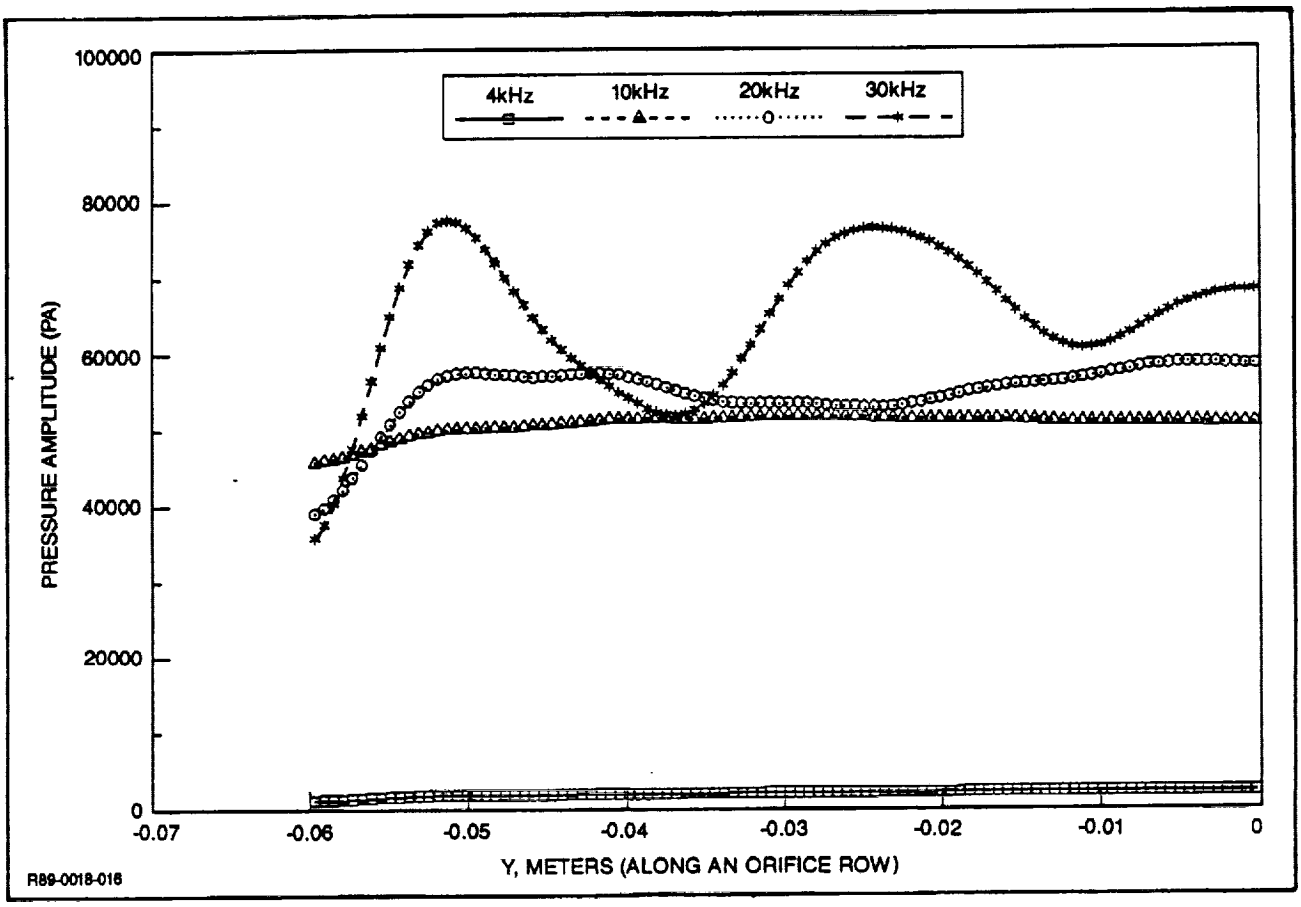

Fig. 16 Acoustic Cavity Pressure at x = 0

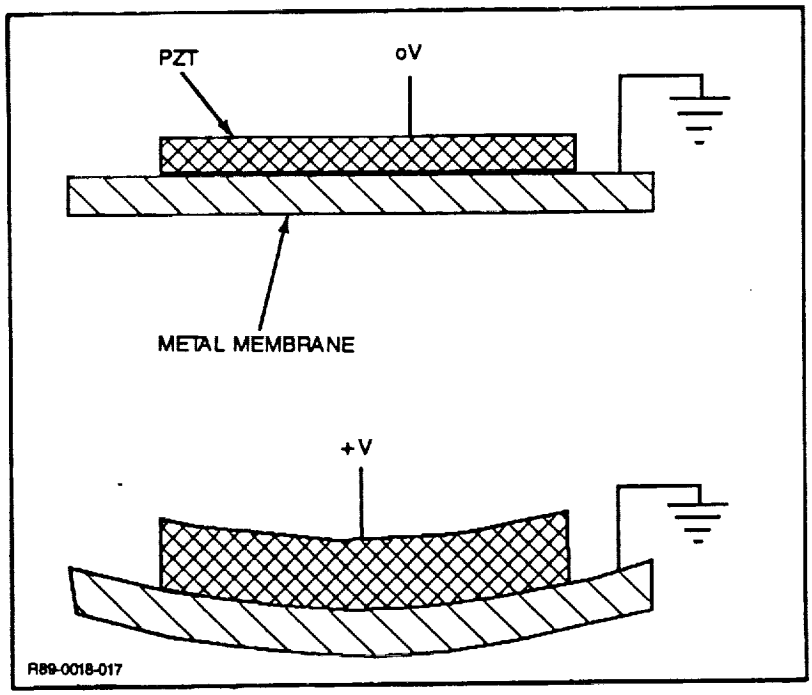

Fig. 17 Bender-Type Transducer Configuration

After analyzing several configurations, the following dimensions for the PZT and metal were chosen: width - 10 cm, PZT thickness - 1 mm, steel thickness - 2 mm. This resulted in a resonant frequency of 36 kHz, a maximum displacement of 0.5 mm , and a maximum (simple wave flow) pressure of 42 kPa. Displacement and pressure vs time are shown in Fig. 18.

Stimulator Performance Estimate

The results of the transducer analysis may be used to estimate the performance of the stimulator. The pressure perturbation required to achieve uniform drop generation is a function of the dynamic pressure. Table 6 shows the jet dynamic pressures and the minimum and maximum perturbation pressures for the four operating conditions.

Although the required perturbation values are still a matter of debate, the values shown should be more than sufficient in most cases. The order of magnitude variation for case 4 indicates that part of the array will be underdriven. Otherwise, the drop generator design appears to have sufficient margin. Note that the 10 kHz values (case 2) are consistent with the values obtained from the simple wave flow analysis.

Collector

Investigations of the various LDR configurations have identified the rectangular and triangular LDR as the most viable for future LDR use (Ref 4 and 17). Figure 3 illustrates both approaches. The basic difference between the two is that the rectangular system uses a linear collector where the droplet streams from each generator are collected by a corresponding collector. With the triangular system, droplet streams from many generator modules are focused on a single centrifugal collector.

Grumman prefers the rectangular system due to its inherently simplistic design and because the focusing of the droplet streams required in the triangular design will decrease its heat transfer capability and may cause fluid loss due to droplet collisions. Unpublished results from McDonnell Douglas, Huntington Beach, and Spectra Technology, Seattle, both proponents of the triangular system, have concluded that the triangular system is lighter weight; an investigation to independently determine the weights of both the LDR systems was conducted.

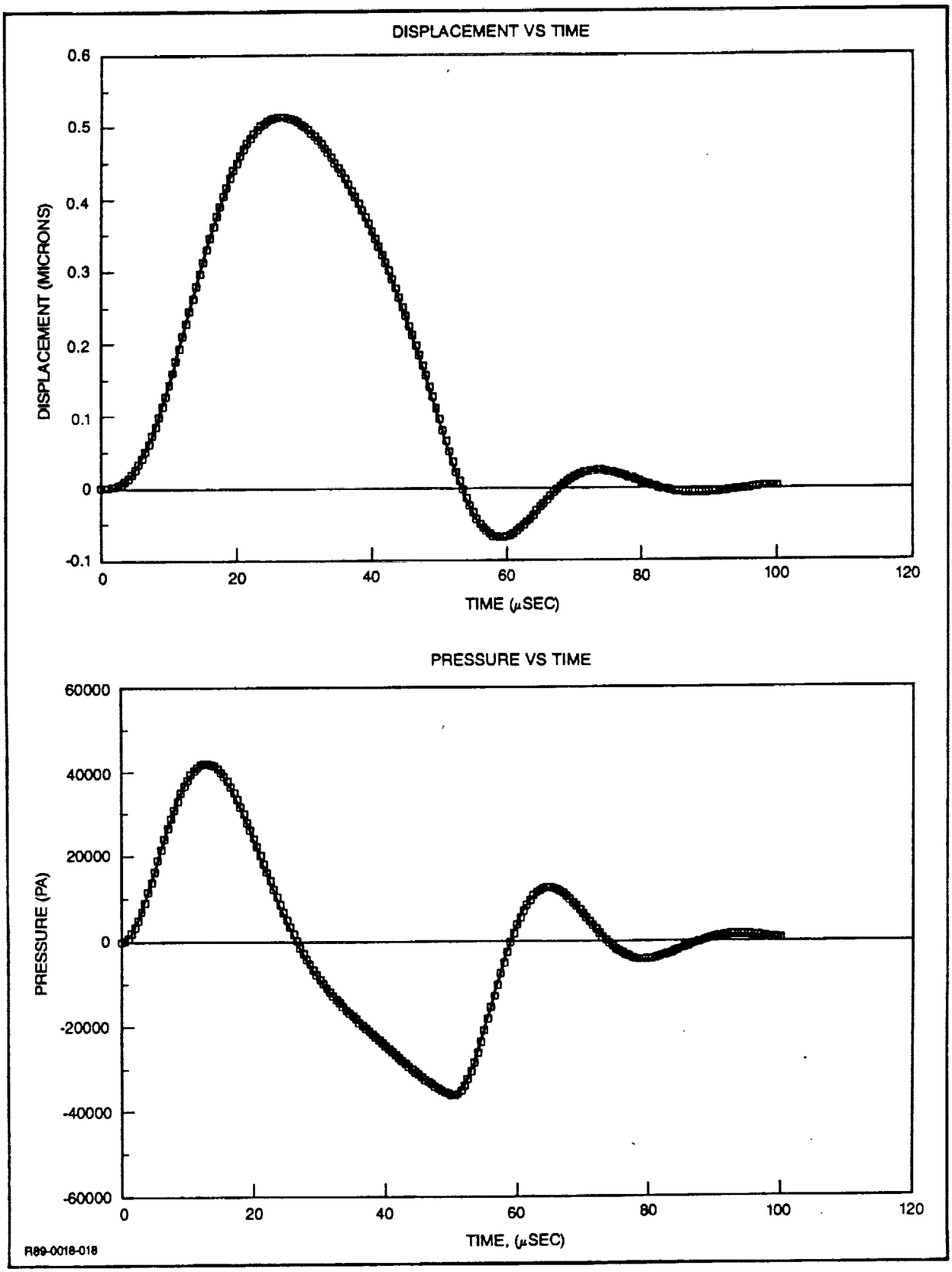

Fig. 18 Transducer Dynamic Analysis Results

Table 6 Jet Dynamic Pressures and Minimum and Maximum Perturbation Pressures for Four Operating Conditions

Case	Dynamic Pressure kPa	Perturbation Pressure		Perturbation/Dynamic Pressure	
		Minimum kPa	Maximum kPa	Minimum %	Maximum %
1	3.5	0.8	2.2	23	63
2	8.6	44	51	512	593
3	31.7	32	58	100	183
4	72.0	6	75	8	104

R89-0018-042

LDR System Analysis Computer Code

The weights of the LDR systems were computed using the liquid droplet radiator system (LDRSYS) analysis computer code. The inputs to the program include: fluid selection, droplet diameter, droplet velocity, pitch/diameter ratios, and number of passes. The code is capable of evaluating rectangular as well as triangular LDR systems. The code computes the heat rejected; temperature at the collector; and the weight of the fluid, generator, collector, deployable mast and the piping. The weights of the components are calculated using the formulae listed in Table A-1 in the Appendix. An example of the program output is shown in Fig. A-1 in the Appendix.

The linear collector weight is based on a conceptual design which uses nylon spur gears mounted on tubular aluminum shafts. In this design, the output pressure from the collector is kept low (approximately 1 psi) in order to minimize the weight required for the gear housing; the fluid pressure is increased downstream from the collector where it can be done more efficiently. The code assumes that the weight of the centrifugal pump for the triangular system is 4.7 kg (10.4 lb) for all cases.

The droplet diameters and pitch/diameter ratio in the velocity direction were selected based on formulae developed in Ref 1. A spreadsheet program was utilized to do a first order approximation of the LDR system dimensions for given heat rejection and temperature requirements.

200 kW System

The 200 kW heat rejection system parameters were chosen based on projected high powered space station requirements. The following assumptions were made concerning the

operating characteristics of the heat rejection system:

- •314°K (106 °F) inlet temperature
- •270°K (27 °F) outlet temperature
- •Dow Corning 704 silicone oil
- •2 msec droplet velocity
- •205 μm droplet diameter
- •0.2 droplet emissivity
- •3.0 averaged pitch/diameter (P/d) (velocity and width directions).

A parametric analysis of the weight of both the rectangular and triangular systems for 5, 10, 20, and 30 droplet layer systems indicate that the optimized rectangular system (20 layers, 494 kg) is 71 kg (157 lb) lighter than the optimized triangular system (5 layers, 565 kg). Using current state-of-the-art heat pipe technology, the heat rejection system would weigh approximately 5100 kg (11,230 lb). Plots of the system weights as a function of number of layers are shown in Fig. 19. Table A-2 in the Appendix gives a weight breakdown of all the system components and details the system length and width requirements.

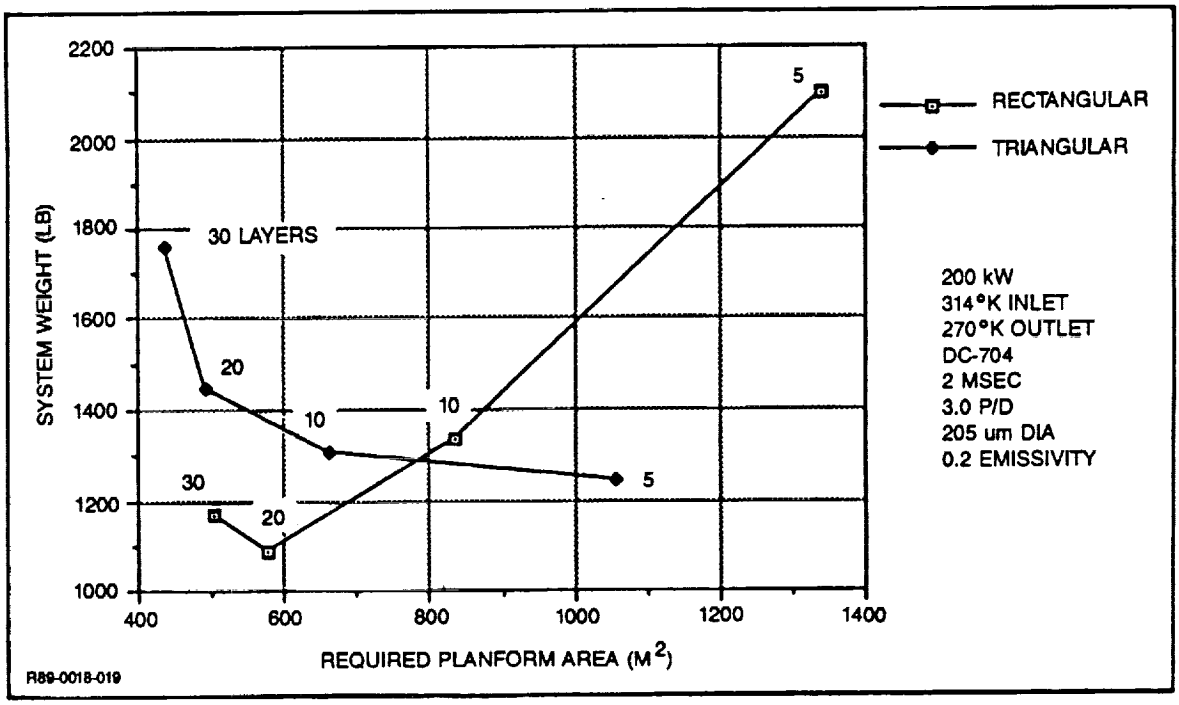

Fig. 19 Rectangular vs Triangular LDR System Weights, 200 kW

3 & 30 MW Systems

The operating characteristics for the 3 and 30 MW LDR heat rejection systems are tabulated below:

3 MW	30 MW
•750°K inlet temperature	•750°K inlet temperature
•550°K outlet temperature	•550°K outlet temperature
•Tin	•Tin
•10 msec droplet velocity	•15 msec droplet velocity
•86 μm droplet diameter	•86 μm droplet diameter
•0.2 droplet emissivity	•0.2 droplet emissivity
•3.0 averaged P/d	•3.0 averaged P/d

The results of the parametric studies are plotted in Fig. 20 and 21. The rectangular system is 165 and 1170 kg (365 and 2575 lb) lighter in weight for the 3 MW and 30 MW systems, respectively. Note that the system weight of the 30 MW triangular system is least when there are 20 layers -- this was not chosen as the optimum case because the required generator width will be unreasonably long (~120 meters). Table A-2 of the Appendix lists the system dimensions and component weights for each of the cases run. Figure 22 compares

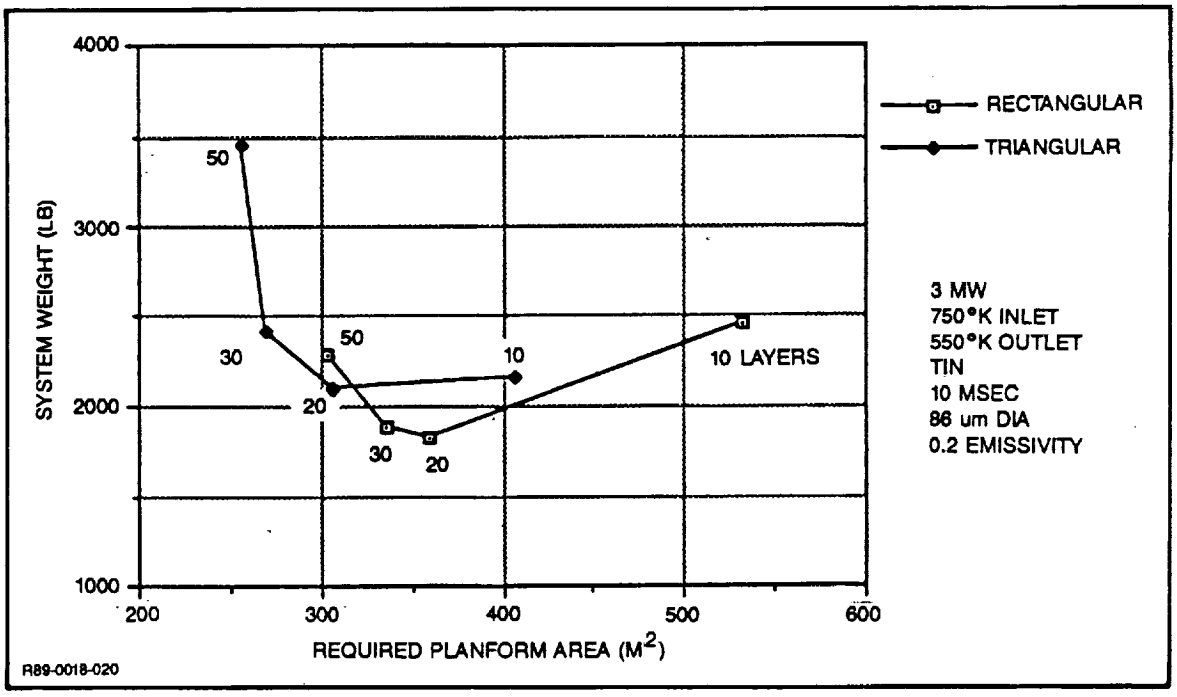

Fig. 20 Rectangular vs Triangular LDR System Weights, 3 MW

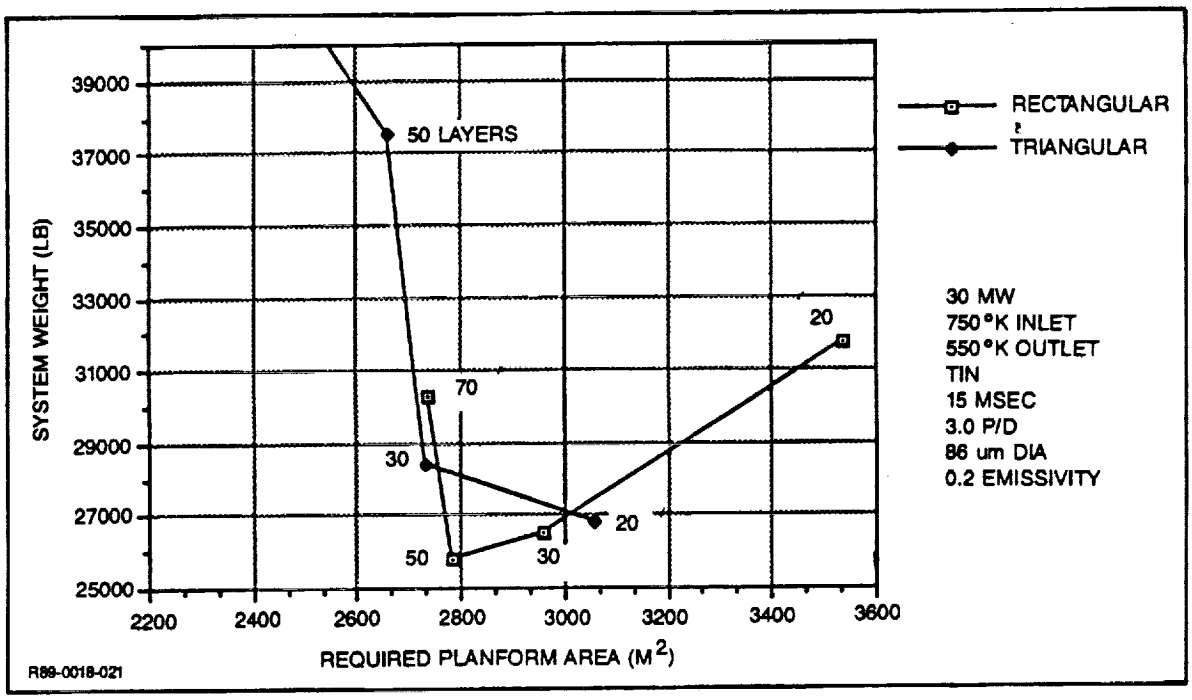

Fig. 21 Rectangular vs Triangular LDR System Weights, 30 MW

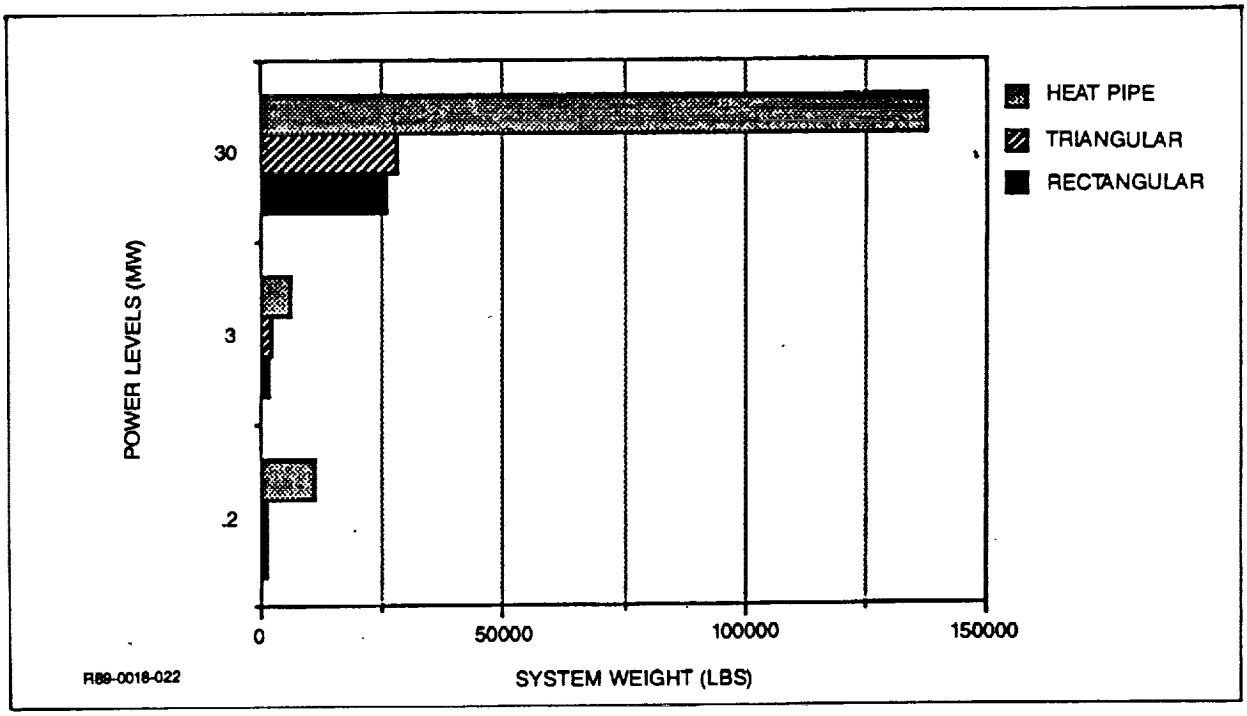

Fig. 22 LDR vs Heat Pipe System Weights

the optimized rectangular and triangular LDR system weights with the weight of a heat rejection system using current heat pipe technology. The 200 kW radiator weight was computed using the current Grumman monogroove heat pipe radiator panel weight 11.7 kg/m^2 (2.4 lb/ft^2); the 3 and 30 MW weights were estimated using predicted weights of a dual-slot heat pipe heat rejection system.

The results of the investigation conclude that rectangular LDR systems weigh less than triangular systems for a range of heat rejection rates and temperature levels. This conclusion is not surprising, since for the same amount of droplet stream weight the triangular system will have half the radiating area of the rectangular system. Although the fluid temperature in the triangular system is at a higher temperature when it has more radiative area and it will have a lighter collector than the rectangular system, this does not obviate the significant increase of fluid mass required in the triangular system compared to the rectangular system. To illustrate this point, Fig. 23 compares the fluid weight of the triangular system with the fluid and collector weight of the rectangular system. The figure clearly shows that, assuming that all the other components of the triangular and rectangular systems (i.e., generator, piping, deployable mast, etc.) are equal in weight, the rectangular system is appreciably lighter than the triangular system.

Effects of Droplet Collisions

As droplet collisions occur along the length of the stream, the effective radiating area of the LDR is decreased. A tradeoff to determine whether it is more desirable to have a larger initial P/d ratio in order to decrease the number of downstream droplet collisions was investigated. The path length, L, required in order to have one droplet collision is predicted by:

$$L = \frac{4}{\pi}\left(\frac{P}{d}\right)^3\left(\frac{d}{\theta_c}\right)$$

where θ_c is the characteristic mean angular divergence, d is the droplet diameter and P is the average pitch of the droplets in width, height and velocity directions. A spreadsheet program was developed to predict the sheet emittance of the droplet streams as a function of droplet collisions. Table 7 illustrates two cases: in case 1 the P/d ratio in the velocity and width direction is 3.0 and the P/d ratio in the thickness direction is 10.0, in case 2 the P/d ratio in the velocity and width directions is 5.0 and 10.0 in the thickness direction. For both cases, the droplet diameter is 205 μm, there are 20 layers, and the divergence is 0.001 rad. Note the P/d ratio in the thickness direction does not affect the sheet emittance (Ref 1). In case 1,

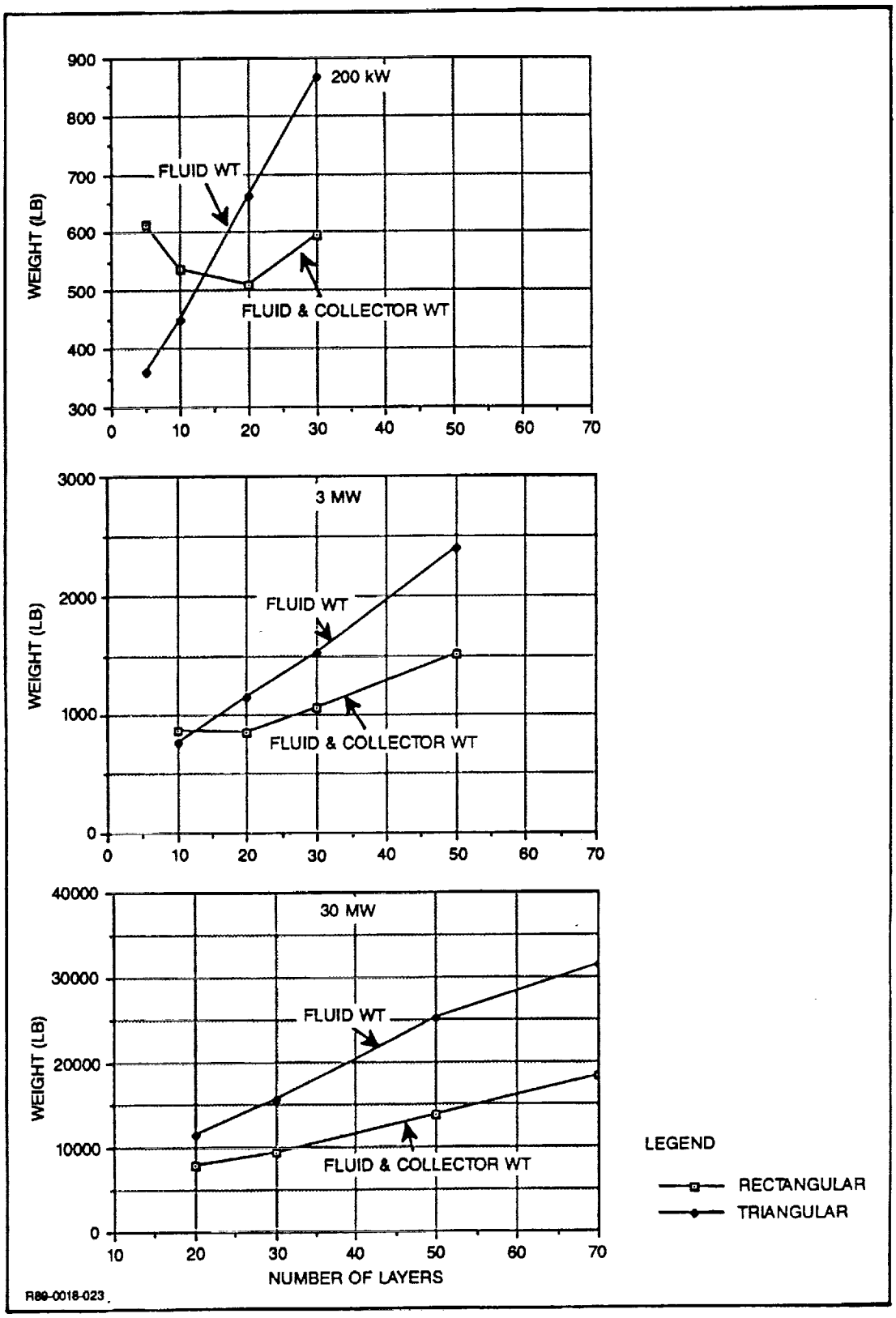

Fig. 23 Fluid Weight Comparison for 0.2, 3, & 30 MW Systems

Table 7 Effect of Initial Pitch/Diameter Ratio on Sheet Emissivity

Case	Droplet Diameter	No. Rows Height	Pitch ht (cm)	Pitch Width (cm)	Pitch Vel (cm)	Mean Driver (rad)	Length (m)	Sheet Emissivity
1	0.02050	20	0.200	0.061	0.061	0.001	22.8438413	0.40
	0.02583	20	0.200	0.184	0.061	0.001	43.1721548	0.31
	0.03254	20	0.200	0.184	0.553	0.001	244.77078	0.04
2	0.02050	20	0.200	0.100	0.100	0.001	60.5943864	0.25
	0.02583	20	0.200	0.300	0.100	0.001	114.516214	0.15
	0.03254	20	0.200	0.300	0.900	0.001	649.266251	0.00

R89-0018-038

the droplets will undergo two collisions: the first collision is predicted to take place 22.8 m from the generator and the second collision, 43.2 m later. The weighted average emittance of the droplet stream is approximately 0.35 for a 50 m sheet length. In case 2, although the droplets will not undergo a collision (the first collision is predicted to take place 60.6 meters from the generator), the sheet emittance will only be 0.25. Thus, it is clearly shown that it is more effective to have as small an initial P/d ratio as possible.

A rough estimate of the effect of a degradation of the effective sheet emissivity due to droplet collisions on both the rectangular and triangular LDR system weights was done for the 0.2, 3 and, 30 MW cases. Both concepts required an increase in the overall length of the droplet sheet; the triangular system required more of an increase than the rectangular system but required less generator length. The systems increased by approximately the same weight. It should be noted that the equation was developed for a rectangular LDR droplet sheet -- a triangular sheet would have more collisions due to increasing droplet density and will therefore have more of a weight penalty.

Collector Design

A side and sectional view of the collector are shown in Fig. 24 and 25, respectively. The droplet streams impinge on the collector throat. The pressure from the droplet streams force the fluid in the collector throat, which is a positive displacement gear pump. One of the major criteria in the design of the collector is to minimize weight. To that end, the diameter of the

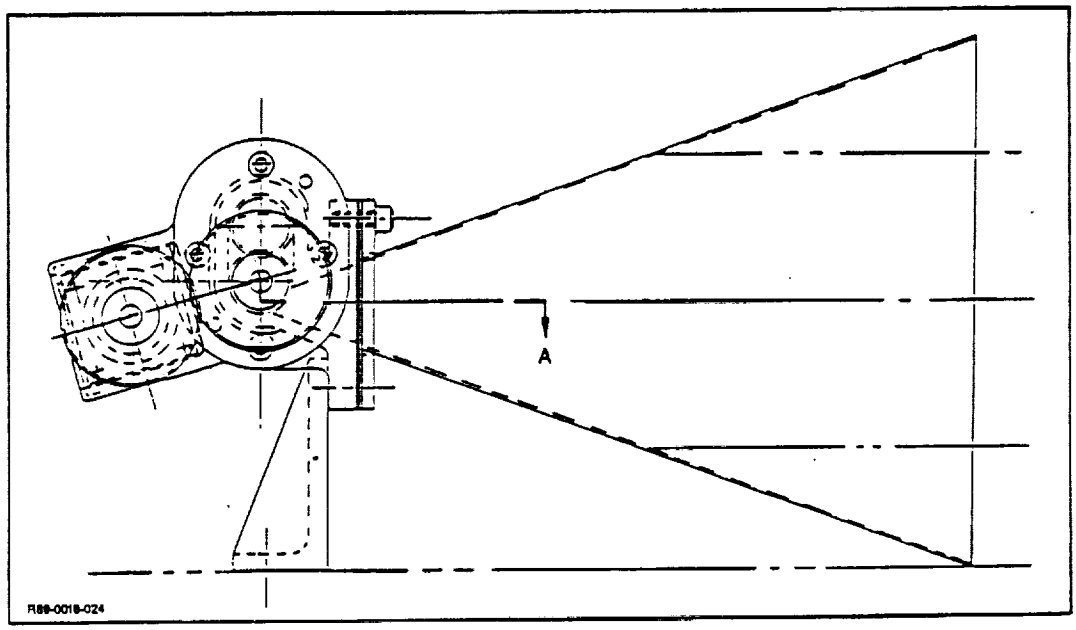

Fig. 24 Side View of Collector

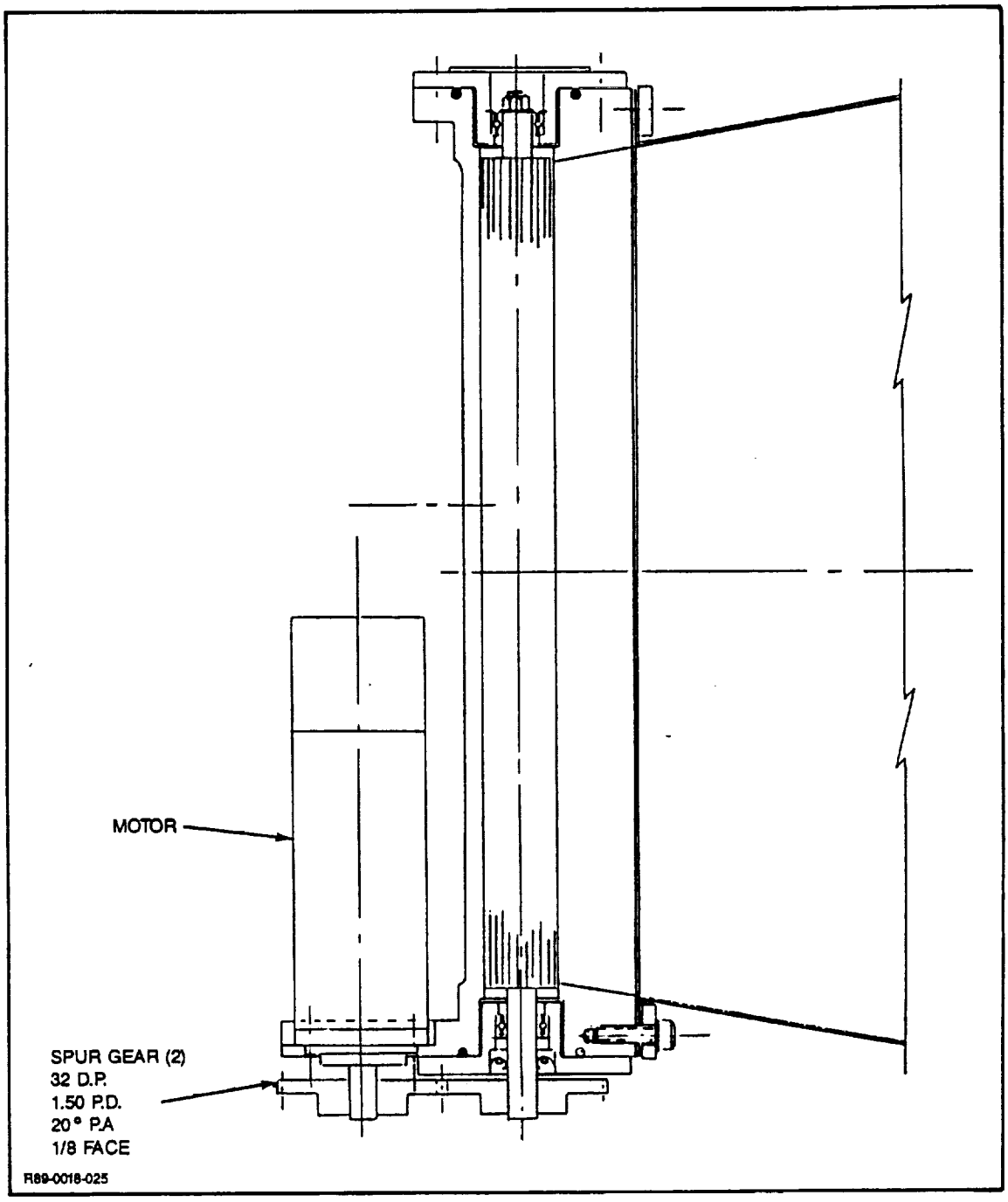

Fig. 25 Sectional View of Collector

spur gears is minimized (1.5 in.) and the output pressure from the collector pump is minimized (1 - 4 psia). A higher output pressure would require a higher gear speed, thicker gear housing, and a larger gear drive motor - all these add weight to the collector. The linear collector weight is approximately 7.61 kg/m (5.1 lb/ft). For a 200 kW LDR system with a 12.2 m collector length, the collector would weigh 93 kg (204 lb).

Optical Loss Detection System

The laser droplet loss detection system will be used to measure the location and rate of droplets falling outside a defined volume. The design includes a two axis droplet-collector alignment error detection scheme which employs a large area quadrant detector and laser beam. Two approaches were investigated. One uses a moving laser beam coupled with a narrow field-of-view tracking detector; the other is static, with a wide field-of-view detector. A comparison of the two systems was made based on issues such as the ability to measure droplet rate, position, size, resolution, and the environmental and packaging issues associated with a space system.

Tracking and non-tracking systems represent the two general approaches used in remote optical detection. The tracking approach includes the comparison of raster and fan beam scan patterns. Common to both these methods are the dependence of the system sensitivity and temporal resolution on the detection method. Three detection schemes were examined as a function of information rate, signal-to-noise ratio, and resolution.

The raster-scanned laser beam configuration, sometimes called LIDAR (light detection and ranging)(Fig. 26) encompasses the functions of the fan and static beam methods. Thus the discussion of Fig. 27 will cover all the component parts investigated. For the purpose of simplicity, only droplets passing through two of the surfaces bounding the generator/collector system will be detected by symmetry. The same number of drops should pass through the other two surfaces in a gravity free environment. The physical volume which will be examined for droplets will be bounded by imaginary planes parallel to the normal stream and spaced about 2 - 3 cm apart. They form a narrow volume along the side and top (referencing the mounting structure as the bottom) of the generator/collector system as shown in Fig. 27. The exact width and height of this channel is a function of the probability of the laser beam intercepting a droplet. The final width will be a function of the tradeoff between the laser beam scan angle and rate.

By viewing in the direction parallel to the normal droplet stream, the geometry aids in reducing unwanted signal returns from the walls of the structure and from the normal droplet stream. In addition, direct and indirect returns from the normal stream should appear beyond the maximum range of the measurement and thus can be discriminated against on a temporal basis. Because of the angle the errant droplets are expected to make with respect to the laser beam, the narrow channel will help to optimize the duration the droplets are

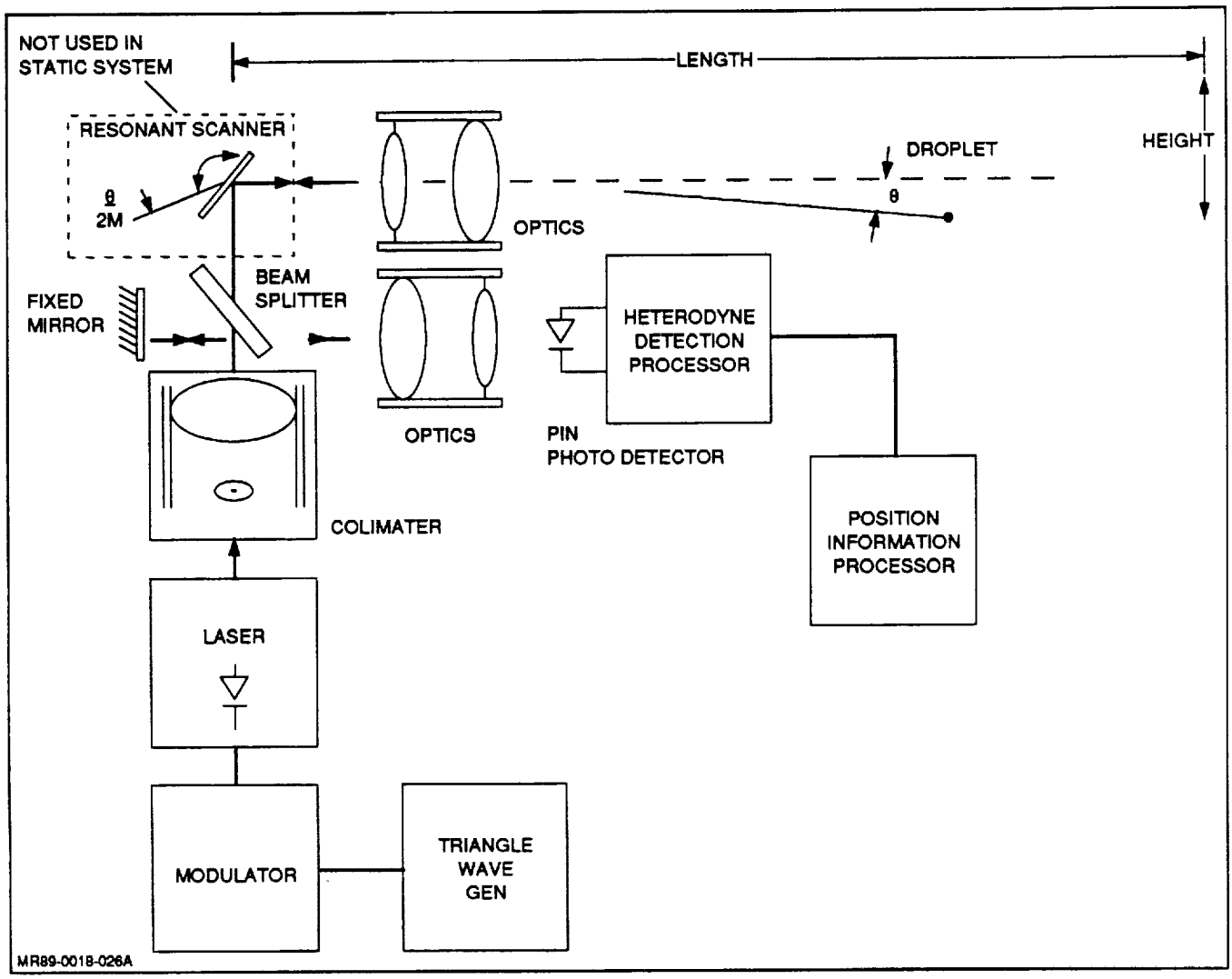

Fig. 26 LIDAR Functional Block Diagram

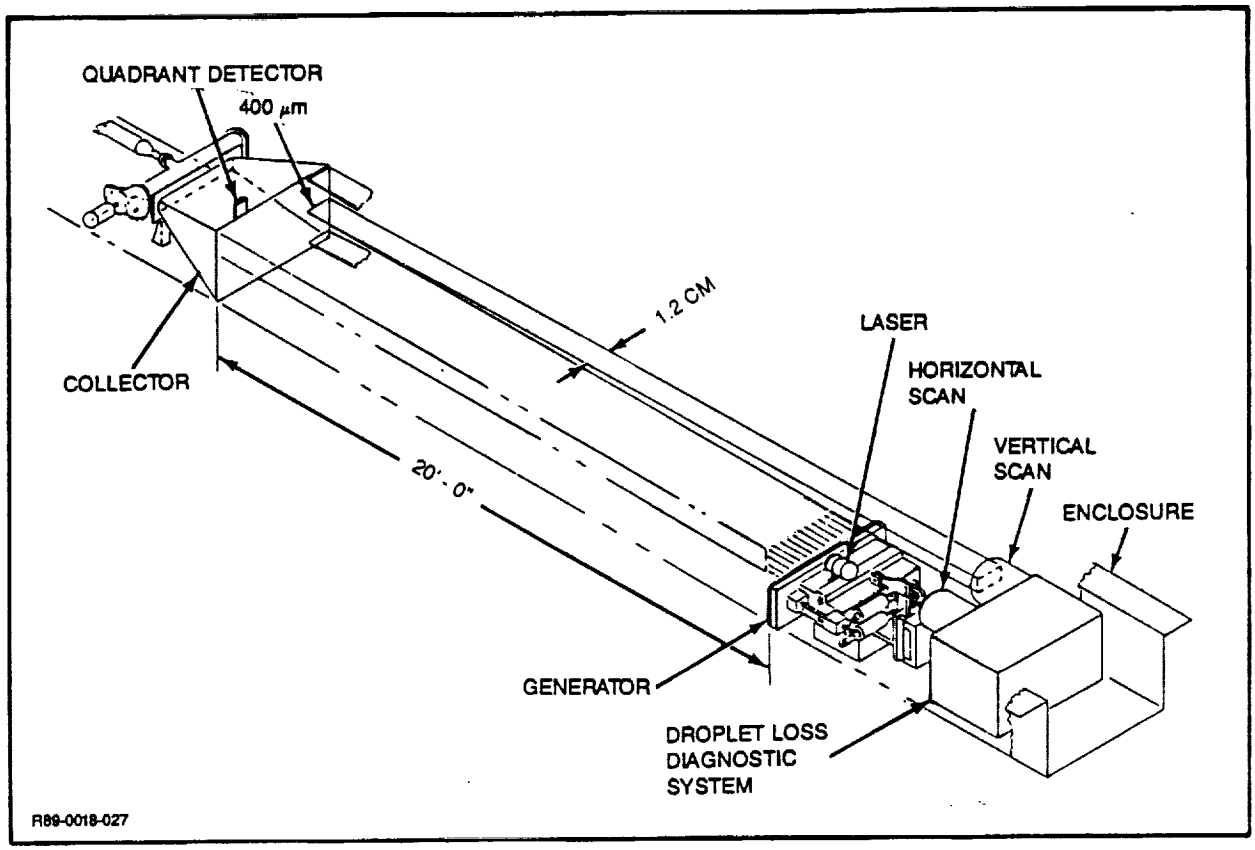

Fig. 27 Laser Droplet Loss Diagnostic System

illuminated. This method of droplet detection can be considered the optical equivalent of a radar where the range information is determined by the modulation and detection scheme.

Three detection and modulation methods were investigated. The differences are basically processing issues which do not impact the packaging considerations, an example of which is lens size and location. The detection methods considered were direct with PIN or avalanche photodetector, photon counting with an avalanche photodiode and pulse height comparator, and heterodyne detection. The modulation methods include picosecond pulse modulation, continuous wave frequency modulation (FMCW), and pulse doppler.

The modulated signal reflected from a droplet is detected by one of the proposed methods to determine range. Angular position is determined from the encoded location of the optical deflector used to develop the raster scan. The fan beam approach will only provide range and angular information in one axis. Since the width of the measuring volume is narrow, this should provide sufficient information about the droplet location.

The static approach takes the form of a narrow curtain of light parallel to the droplet path generated by a multiple of lasers and receiver pairs. Each optical pair will look along a different section parallel to the normal droplet path. Range (distance) will be measured as in the scanning system, with the section location determined by sampling the outputs. Schematically this approach will look similar to that presented in Fig. 26, but without the scanning section.

The alignment system will be based upon a collimated laser source pointing at a quadrant photodetector. The laser is mounted on the generator and the detector is mounted on the collector. By vectorially summing the signals from each of the detector quadrants, the magnitude and direction of the displacement is determined and converted to an error voltage (with magnitude and direction information) for each of the two axes. The limiting factor on the range of the alignment system is the linear displacement that can be accommodated by the detector. Typically a single quadrant detector can detect a linear displacement of up to +/- 1/4 in. For greater displacements a combination of linear detectors will be required. These signals are used by the servo system to correct for displacements in the droplet generator/collector structure.

The error signals also provide the LIDAR with information about the change in position of the droplet generator with respect to the collector. In the scanning approach this permits the scan to be automatically adjusted so the laser beam is always pointing parallel to the normal droplet stream. In the fixed beam approach it may be simpler to just attach the detection system to the generator housing.

6 – PAYLOAD ACCOMMODATION

One of the key goals in the design of the LDR experiment was to make its integration into the shuttle bay as simple and as straightforward as possible. To do this, all of the aspects of the integration - structural, dynamic, data handling, control, and power - are all kept within the constraints of standard shuttle experiments.

In order to design an experiment that will demonstrate an extremely low droplet loss rate (i.e., $1{:}10^8$), it is necessary that the generator-to-collector path length be long and that there be a diagnostic system which will detect any LDR droplets that stray outside the permissible envelope. The Grumman shuttle-attached space station heat pipe advanced radiator element (SHARE) experiment which flew in March 1989 aboard the Space Shuttle Discovery and the proposed space radiator assembly demonstration (SRAD) experiment both have similar payload dimensional requirements - namely, a long aspect ratio. The experiment is positioned in the shuttle bay opposite the shuttle's remote manipulator arm within a 38.1 cm (15 in.) diameter envelope, as shown in Fig. 28.

The LDR experiment will be mounted onto a beam similar to the beam used on the SHARE experiment. With 594 kg (270 lb) of heat pipe radiators attached to the SRAD beam has been designed to handle the shuttle induced loads through ascent and descent with 594 kg (270 lb) of heat pipe radiators attached to it. The LDR experiment is estimated to weigh 73 kg (160 lb). The flight path of the droplets will be 6.1 m (20 ft) and the entire experiment will fit within a 38.1 cm (15 in.) diameter dynamic envelope. The 6.1 m generator-to-collector path length was chosen assuming that the angular divergence of the droplet streams will not exceed 5 mrad. Using this path length, the droplet streams come close to the walls of the enclosure which encapsulates the experiment. The overall length of the LDR experiment, including all auxiliary equipment, will be approximately 9.1 m (30 ft).

Figure 29 details a cross-section of the LDR enclosure. The enclosure which encapsulates the experiment is a leak-tight structure manufactured out of 0.102-cm (0.040-in.) thick sheet aluminum with ribs every 12 in. The pressure changes induced during shuttle ascent and descent are a major consideration in the design of the LDR enclosure. Figure 30 details these changes during shuttle launch (Ref 8). The pressure change between the shuttle bay and the LDR enclosure is controlled with a series of check valves and solenoid latch valves. The enclosure is designed so that the the maximum pressure differential between the inside of the enclosure and the shuttle bay does not exceed 0.5 psi.

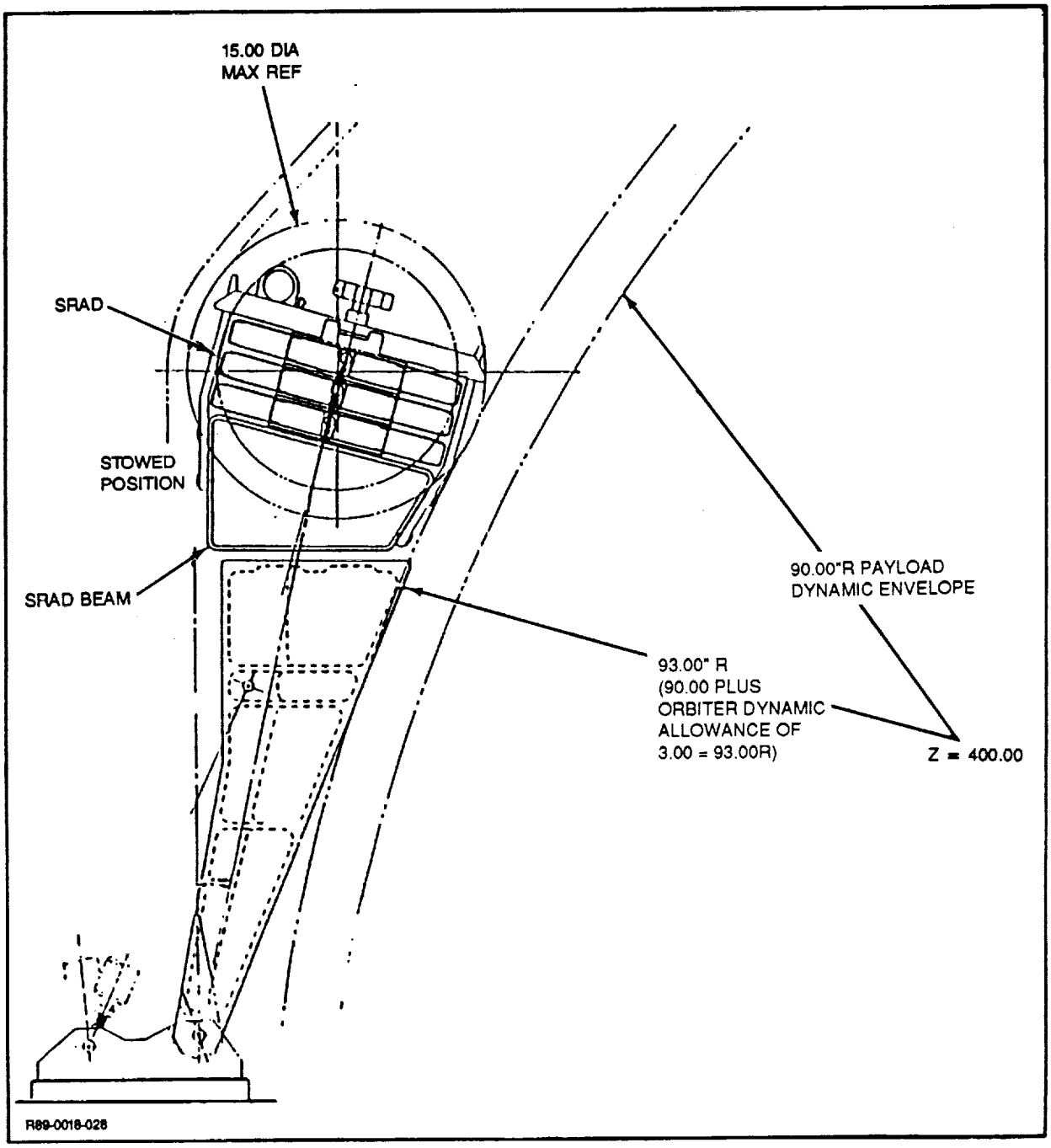

Fig. 28 Location of LDR Experiment

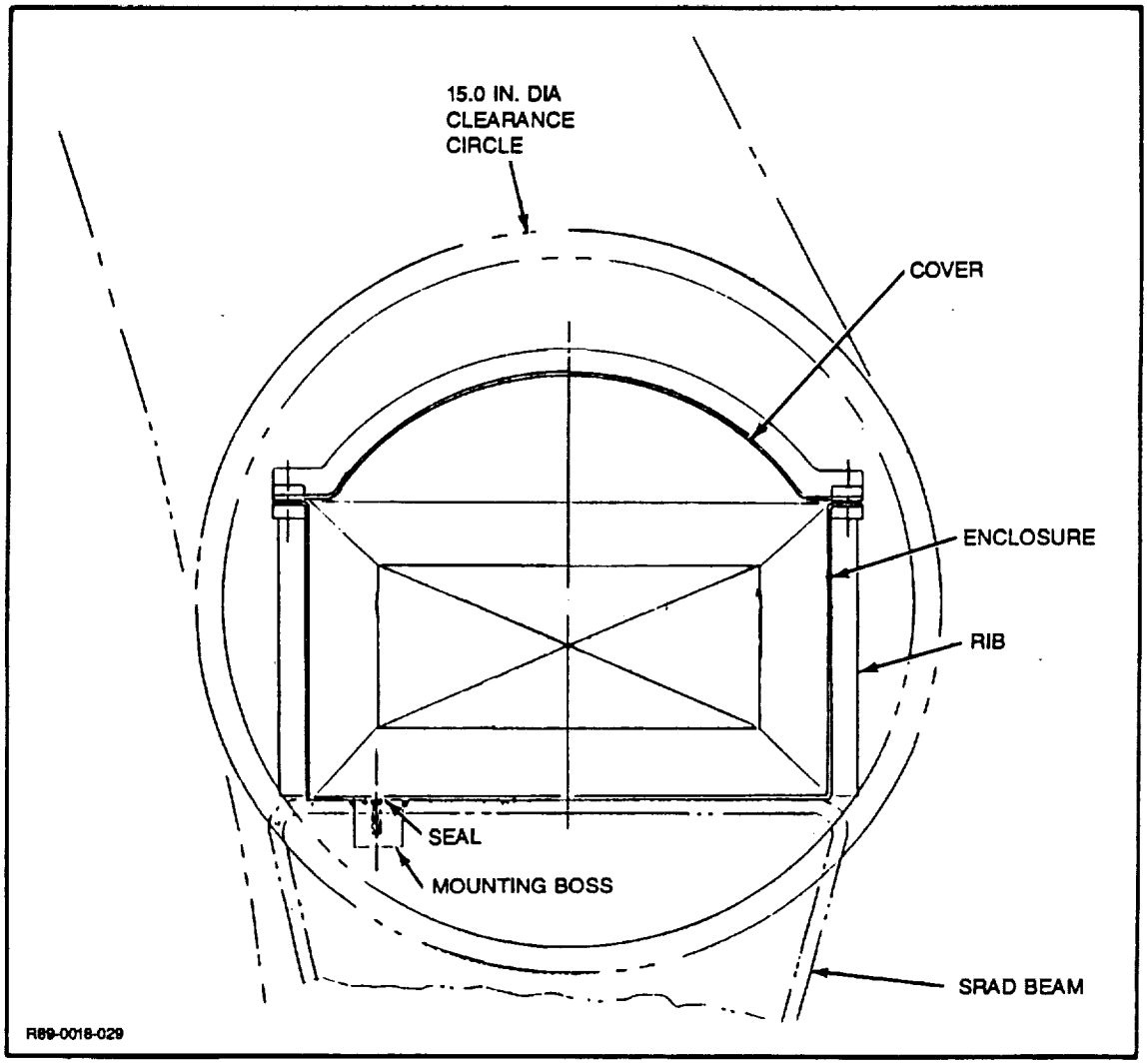

Fig. 29 Cross-Section of LDR Enclosure

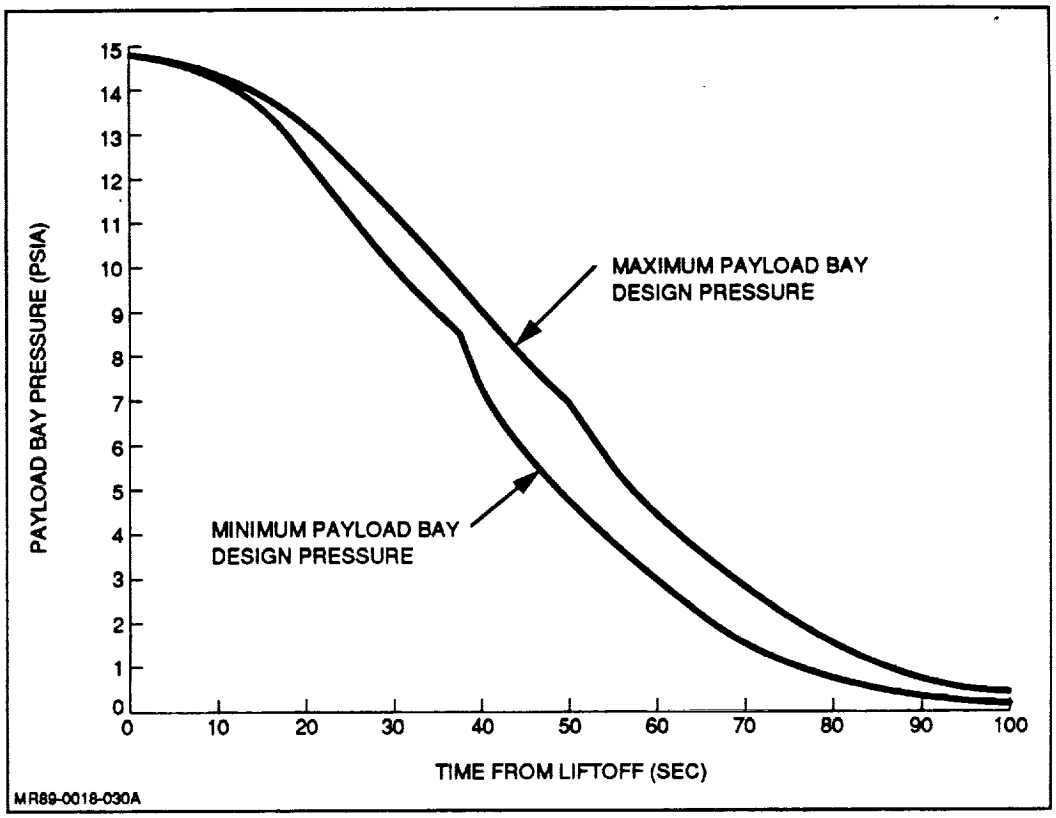

Fig. 30 Pressure History of Shuttle Bay After Liftoff

The experiment is designed to be integrated into the shuttle bay and to operate using standard shuttle experiment electrical power - 28 Vdc and 1750 W continuous, 3000 W peak. It is estimated that the maximum power requirements for the LDR experiment will be less than 1200 W continuous power.

The effect of the shuttle accelerations on the droplet generator-to-collector path was investigated. Reference 8 details the maximum accelerations that can be expected from the shuttle's vernier reaction control system. Preliminary results of the investigation show that under worst-case conditions the droplets will only deviate from their paths by a maximum of 0.8 in. in any direction. Thus, the experiment can operate through all the vernier accelerations. The LDR will not be able to operate during main thruster acceleration; these accelerations normally take place once every 4.5 hr (Ref 8).

Crew Involvment

The LDR experiment will be controlled via an astronaut/ground station link. The astronaut will use the standard switch panel (SSP), illustrated in Fig. 31, to control all the vital

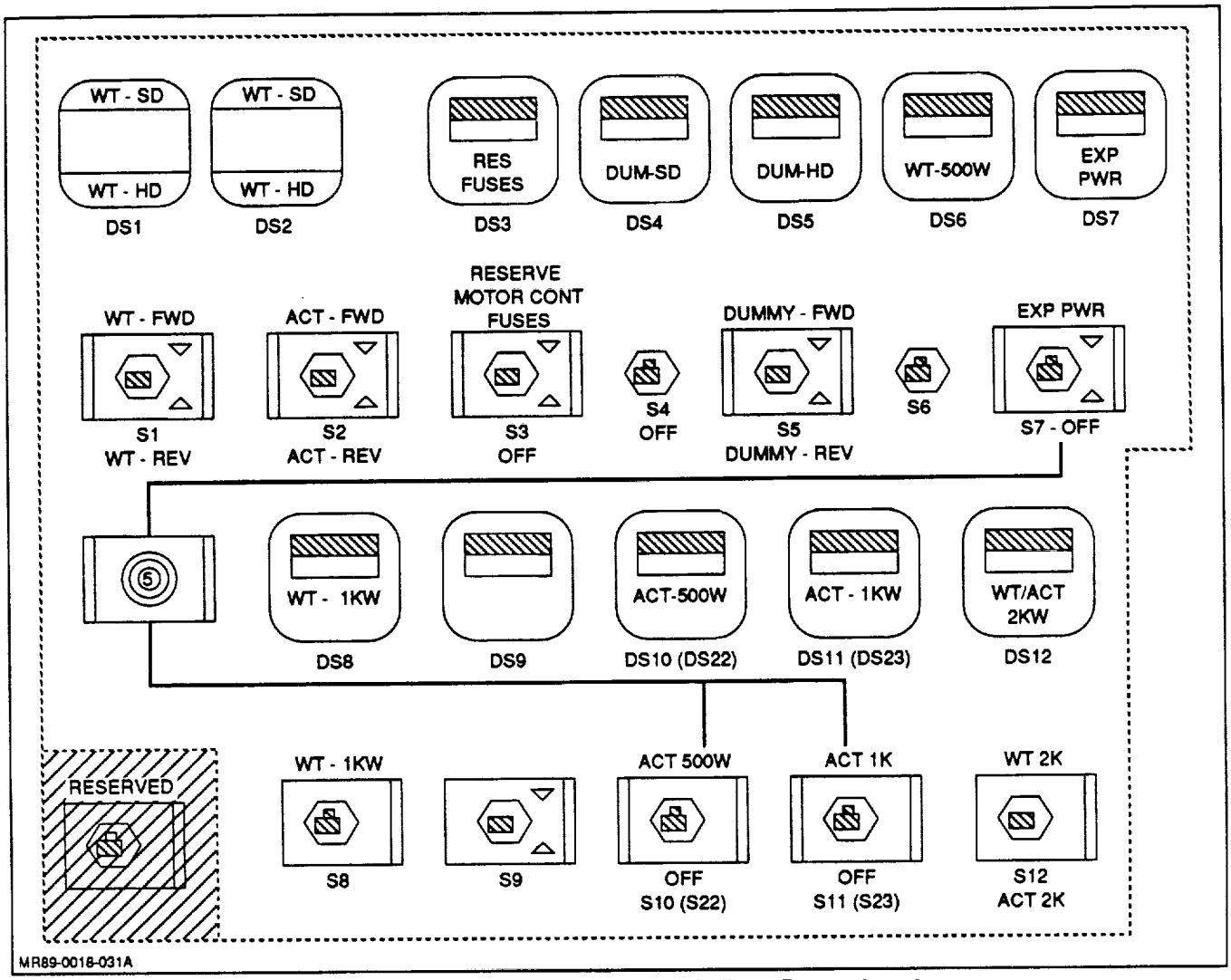

Fig. 31 Standard Switch Panel Shuttle Crew Compartment

functions of the experiment. The astronaut will receive support and direction from the ground station and will monitor the experiment throughout its estimated 3-hr duration. The experiment can be automated so that little or no astronaut intervention is necessary; however, this would significantly increase the complexity and cost of the experiment.

7 – COST & IMPLEMENTATION PLAN

The cost and schedule for a follow-on LDR engineering development contract is shown in Fig. 32. The effort includes detailed engineering development of an LDR experiment and the ground test of any LDR component that requires a ground test to demonstrate feasibility. The cost estimate assumes that the orifice plate and generator will be manufactured from components that will be available from the NASA Contract NAS3-25275. The generator will be modified in order to integrate the shear seal valve.

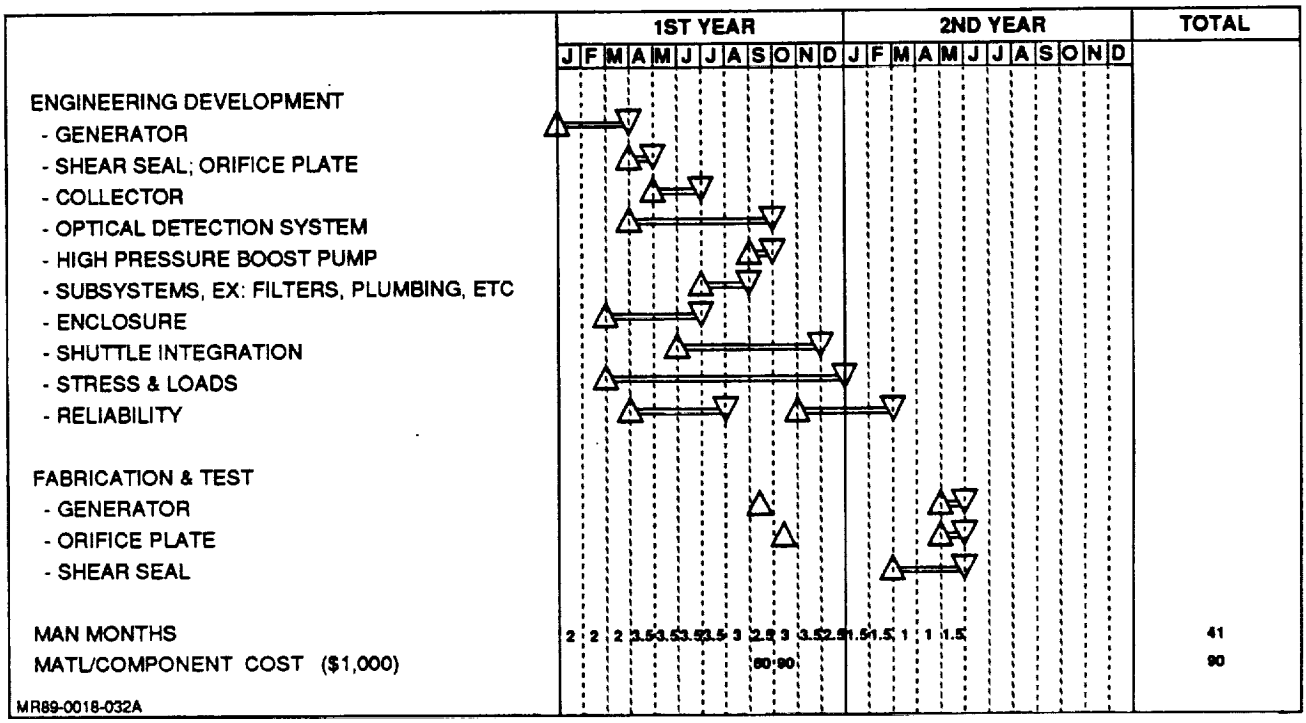

Fig. 32 LDR Cost & Implementation Plan

8 – CONCLUSIONS

A conceptual design of a LDR shuttle-attached experiment has been developed. The purpose of the experiment is to investigate physical phenomena that cannot be adequately tested in a 1g or transient 0g environment. All major components of an LDR system are integrated into the experiment. A major thrust in the design of the experiment was that representative subsections of a 'full-up' system could be investigated.The droplet generator system is acoustically driven and operates between 4 - 30 kHz. The fluid is Dow Corning 704 silicone oil. Two different droplet collection schemes were compared: the centrifugal approach and the linear collection scheme. On the basis of simplicity, reliability and weight, the linear collector method was selected for the conceptual design. The droplet loss detection system uses a moving laser beam coupled with a narrow field-of-view tracking detector to detect stray droplets.

The LDR experiment is estimated to weigh 73 kg (160 lb), be 9.1 m (30 ft) long, and fit within a 38.1 cm (15 in.) diameter. The experiment is designed to be integrated into the shuttle bay using standard shuttle/experiment power, weight, and data requirements.

9 – REFERENCES

1. Brown, R.F. and Kosson, R., "*Liquid Droplet Radiator Sheet Design Considerations,*" *Advanced Energy Systems - Their Role in Our Future, Vol. 1,* American Nuclear Society, 1984

2. Hertzberg, A. and Mattick, A.T., *New Thermal Management and Heat Rejection Systems for Space Applications,* AFRPL TR-85-080, 1984

3. Mankaymer, M.M., et. al., *Liquid Droplet Radiator System Investigation,* AFRPL TR-85-080, 1985

4. White, K. A., *Liquid Droplet Radiator Development Status,* AIAA-87-1537, June 1987

5. Grumman Aerospace, *Liquid Droplet Radiator Collector Component Development,* AFRPL TR-85-082, 1985

6. Solon, M., et. al., *Space Power Heat Rejection System Trades for the Strategic Defense Initiative,* DOE Contract No. DE-AC03-865F/1601, December 1987

7. Calia V., et. al., "Liquid Droplet Radiator Collector Development," *Advanced Energy Systems - Their Role in Our Future, Vol. 1,* American Nuclear Society, 1984

8. *Shuttle/Payload Interface Definition Document for Standard Accommodation,* JSC 21000-1DD-STD, November 1985

9. Bush, J. M., Hayes, D.J., and Wallace, D. B.,*Study of Orifice Fabrication Technologies for the Liquid Droplet Radiator,* NASA Contract NAS3-25275 to be published as NASA Contract Report, 1990

10. Hertzberg, A. and Mattick, A.T., "Liquid Droplet Radiator Technology Issues," *Space Nuclear Power System 1984,* Edited by El-Genk, M.S.and Hoover,M.D., Orbit Book Co., Malabar, FL ,1985.

11. Mattick , A.T. and Taussig, R.T., *New Thermal Management and Heat Rejection Systems for Space Applications,* AFRPL Report TR-84-039, June, 1984.

12. Goren, S.L. and Wronski, S.,"The Shape of Low-Speed Capillary Jets of Newtonian Liquids," *J. Fluid Mech.*, Vol 25, Part 1, pp 185 - 198, 1966.

13. Omodei, B.J., "Computer Solutions of a Plane Newtonian Jet with Surface Tension," *Computers and Fluids*, Vol 7, pp 79 - 96, 1979.

14. Arista, G. and Greco, G., "Excess Pressure Drop in Laminar Flow Through a Sudden Contraction," *Ind. Eng. Chem. Fundamentals,* Vol 7, pp 595, 1968.

15. Kaye, S.E. and Rosen, S.L., "The Dependence of Laminar Entrance Loss Coefficient on Contraction Ratio for Newtonian Fluids," *Amer. Inst. Chem. Eng. J.*, Vol 17, pp 1269, 1971.

16. Rosen, S.L. and Sylvester, N.D., "Laminar Flow in the Entrance Region of a Cylindrical Tube," *Amer. Inst. Chem. Eng. J.*, Vol 16, pp 964, 1970.

17. Mattick, A.T. and Taussig, R.T. , *New Thermal Management and Heat Rejection Systems for Space Applications,* AFRPL Report TR-84-039, June, 1984.

18. Wallace, D.B., *Performance Charteristics of a Drop-on-Demand Ink Jet Device,* Ph.D. Dissertation, The University of Texas at Arlington, December, 1987.

19. Muntz, E.P., et. al., *Liquid Droplet Generation,* NASA CR-182246, 1988

Appendix

Liquid Droplet Radiator System Analysis Computer Code

Table A-1 Estimated Weight Breakdown of LDR Components

Generator:	18.04 lb/m
Collector:	10.40 lb/m (rectangular)
Deployable Mast:	1.95 lb/m
Piping Weight:	$\pi \varrho p$ Dt L_p
Pipe Thickness:	0.01 (D)
Fluid Weight:	1.25 weight of fluid sheet plus weight of fluid in piping
Contingency Weight:	(0.2) total weight

R89-0018-040

Mass flow rate = 2.9100E+00 kg/sec

Pass 1

Length (m)	Sheet Thickness (°K)	Average Temperature (In.)	Heat Rejected (w)	Evap Rate (kg/yr)	Effective Sheet Emissivity
0.0	0.4843	314.00	0.00E+00	0.0	0.4105
4	0.7992	311.73	1.105E+04	1.9	0.4105
8	1.1142	309.52	2.179E+04	3.2	0.4105
12.0	1.4291	307.37	3.222E+04	4.2	0.4105
16.0	1.7441	305.28	4.237E+04	4.8	0.4105
20.0	2.0591	303.25	5.224E+04	5.3	0.4105
24.0	2.3740	301.27	6.185E+04	5.7	0.4105
28.0	2.6890	299.34	7.122E+04	5.9	0.4105
32.0	3.0039	297.47	8.035E+04	6.1	0.4105
36.0	3.3189	295.63	8.92E+04	6.3	0.4105
40.0	3.6339	293.85	9.793E+04	6.4	0.4105
44.0	3.9488	292.10	1.064E+05	6.4	0.4105
48.0	4.2638	290.40	1.147E+05	6.5	0.4105

Pass 2

Length (m)	Sheet Thickness (In.)	Average Temperature (°K)	Heat Rejected (w)	Evap Rate (kg/yr)	Effective Sheet Emissivity
0.0	0.4843	290.40	1.147E+05	6.5	0.4105
4.0	0.7992	288.74	1.228E+05	6.5	0.4105
8.0	1.1142	287.11	1.307E+05	6.6	0.4105
12.0	1.4291	285.52	1.384E+05	6.6	0.4105
16.0	1.7441	283.97	1.459E+05	6.6	0.4105
20.0	2.0591	282.44	1.533E+05	6.6	0.4105
24.0	2.3740	280.96	1.606E+05	6.6	0.4105
28.0	2.6890	279.50	1.667E+05	6.6	0.4105
32.0	3.0039	278.07	1.746E+05	6.6	0.4105
36.0	3.3189	276.67	1.814E+05	6.7	0.4105
40.0	3.6339	275.30	1.881E+05	6.7	0.4105
44.0	3.9488	273.96	1.946E+05	6.7	0.4105
48.0	4.2638	272.64	2.010E+05	6.7	0.4105

Pipe-1 diameter = 0.7579 in.
Pipe-2 diameter = 0.5359 in.

Generator weight	=	220.2 lb	99.8 kg
Collector weight	=	126.9 lb	575. kg
Sheet fluid weight	=	385.0 lb	174.6 kg
Piping fluid weight	=	7.8 lb	3.6 kg
Astromast weight	=	187.5 lb	85.0 kg
Piping weight	=	2.3 lb	1.0 kg
Contingency weight	=	185.9 lb	84.3 kg
Total weight	=	1115.6 lb	505.9 kg

Total system weight = 1.11556E+03 lb
Heat rejected/weight = 3.97267E-01 kw/kg
Weight/heat rejected = 2.51720E+00 kg/kw

R89-0018-039

Fig. A-1 Sample Output of LDRSYS Computer Program

Table A-2 LDR Length, Width, Area, and Breakdown

	Planform Area	Length	Width	No. Layers	Generator Weight	Collector Weight	Sheet Fluid Wt	Pipe Fluid Weight	Mast Weight	Total Weight
200 kW										
Rectangular	1340	27.7	48.6		877	505	223	31.1	108	2098
	836	34.6	24.2	10	436	251	286	15	135	1336
	577	47.5	12.2	20	220	126	385	7.8	185.5	1087
	505	62.3	8.1	30	146	84	511	5.2	243	1168
Triangular	1056	4	48		392	10.4	362	15.5	195	1244
	661	8	22.8	10	411	10.4	449	7.1	230	1310
	492	2	12	20	216	10.4	662	4.1	321	1448
	436	109	4	30	144	10.4	867	2.8	425	1762.8
3 MW										
Rectangular	532	15	35.5	10	640	369	499	472	58.6	2471
	360	20	18	20	324	187	675	243	78.1	1822
	336	28	12	30	216	124	945	162	109	1877
	304	40	7.6	50	137	79	1425	108	156	2292
Triangular	407	22	37	10	667	10.4	763	263	112.2	2188
	306	34	18	20	324.8	10.4	1147	128	137.4	2099
	270	45	12	30	216	10.4	1519	87	175.8	2416
	256	64	8	50	144	10.4	2400	67	250	3450
30 MW										
Rectangular	3540	30	118	20	2129	1227	6639	15668	117.2	31740
	2960	37	80	30	1443	832	8439	10802	146	26550
	2784	58	48	50	866	499	13165	6481	228	28821
	2736	72	38	70	685	395	17959	5687	281	30302
Triangular	3060	51	120	20	2165	10.4	11477.9	8169	199	26845
	2730	65	84	30	1515	10.4	15596.4	6025	257	28396
	2660	95	56	50	1010	10.4	25206	4489	375	37540
	2400	120	40	70	721	10.4	31507	3229	468	43291
Lengths (meters) Weights (lb)										

R89-0018-041

NASA
National Aeronautics and Space Administration

Report Documentation Page

1. Report No.	2. Government Accession No.	3. Recipient's Catalog No.
NASA CR-185164		

4. Title and Subtitle	5. Report Date
Conceptual Design of Liquid Droplet Radiator Shuttle-Attached Experiment Final Report	October 1989
	6. Performing Organization Code

7. Author(s)	8. Performing Organization Report No.
Shlomo L. Pfeiffer	
	10. Work Unit No. 506-48-4A

9. Performing Organization Name and Address	11. Contract or Grant No.
Grumman Space Systems Bethpage, NY 11714	NAS3-25357
	13. Type of Report and Period Covered
12. Sponsoring Agency Name and Address	Contractor Report, Final
NASA Lewis Research Center 21000 Brookpark Rd. Cleveland, OH 44135	14. Sponsoring Agency Code

15. Supplementary Notes

Project Manager, Alan White, Power Technology Division,
NASA Lewis Research Center.
In-Space Experiments Focal Point, Olga Gonzalez-Sanabria.

16. Abstract

The conceptual design of a shuttle-attached liquid droplet radiator (LDR) experiment is discussed. The LDR is an advanced, lightweight heat rejection concept that can be used to reject heat from future high powered space platforms. In the LDR concept, submillimeter-sized droplets are generated, pass through space, radiate heat before they are collected, and recirculated back to the heat source. The LDR experiment is designed to be attached to the shuttle longeron and integrated into the shuttle bay using standard shuttle/experiment interfaces. Overall power, weight, and data requirements of the experiment are detailed. The conceptual designs of the droplet radiator, droplet collector, and the optical diagnostic system are discussed in detail. Shuttle integration and safety design issues are also discussed.

17. Key Words (Suggested by Author(s))	18. Distribution Statement
Space Power; Liquid Droplet Radiator; Space Radiator; Shuttle Experiment	Unclassified – Unlimited Subject Categories 18, 20

19. Security Classif. (of this report)	20. Security Classif. (of this page)	21. No of pages	22. Price*
Unclassified	Unclassified	57	A04

NASA FORM 1626 OCT 86

*For sale by the National Technical Information Service, Springfield, Virginia 22161